GEOLOGICA CARPATHICA, 2026, 77, 1, 43–64 https://doi.org/10.31577/GeolCarp.2026.03

Temporal shift in ultrastructure of hyaline calpionellids and their diagenetic modification in the Tithonian–Berriasian pelagic limestones (Western Carpathians)

DIANA ÖLVECZKÁ[1,✉] and ADAM TOMAŠOVÝCH[1]

[1]Earth Science Institute, Slovak Academy of Sciences, Dúbravská cesta 9, 841 04 Bratislava, Slovakia

(Manuscript received October 30, 2025; accepted in revised form February 10, 2026; Associate Editor: Natália Hudáčková)

Abstract: Temporal changes in the composition and ultrastructure of hyaline walls of calpionellids during the Late Jurassic, coinciding with the massive increase of abundance of calcareous nannoplankton and with the onset of maiolica and biancone deposition, are poorly known. Here, we investigate the microtexture of pelagic deposits and the preservation, ultrastructure and chemical composition of three calpionellid genera in the upper Tithonian–lower Berriasian of the Kysuca–Pieniny and Orava successions (Pieniny Klippen Belt, Western Carpathians), using scanning electron microscopy (SEM), backscattered electron imaging (BSE), and wavelength-dispersive spectroscopy (WDS). The microtexture of these facies consists of interlocked pelagic skeletal remains and micritic or microsparitic pore-filling cements. Low-Mg calcitic calpionellid loricae and nannofossils are affected by (1) small-scale dissolution, which causes irregular and locally very thin wall thickness of loricae and (2) aggrading neomorphism, which produces coarser lorica crystals and results in the loss of inter-crystalline boundaries relative to the original lorica ultrastructure. In spite of these diagenetic effects, calpionellid genera differ in their test ultrastructure. Crystals in the hyaline layer of *Praetintinnopsella* and *Crassicollaria* are ~1 μm long and almost equidistant (length/width ratio ~1.3), whereas in *Calpionella,* they are ~2.2 μm long, more elongated (length/width ratio ~2), and oriented perpendicularly or obliquely to the inner surface of the lorica. The ultrastructure of the *Praetintinnopsella* hyaline layer more closely resembles that of *Crassicollaria* that of *Calpionella,* indicating a calcification trend characterised by the formation of larger crystals with lower surface area-to-volume crystal ratio. The loricae of these genera are enriched in Mg and S and impoverished in Mn relative to surrounding micritic and microsparitic grains. The initial diagenetic phase was represented by (1) dissolution of micro- and nannoplankton calcitic remains, (2) by precipitation of micritic and microsparitic cements within pore spaces among uncompacted skeletal particles and inside loricae, and (3) release of Mg from echinoderms coupled with microdolomite precipitation within ossicles or along syntaxial rims. This stage was followed by a phase with small-scale aggrading neomorphism, and ultimately by a late-diagenetic phase characterized by the precipitation of authigenic quartz and albite. Although dissolution, cementation and neomorphism probably reduced abundance of identifiable micritic fraction and abundance of dissolution-sensitive nannofossils, diagenesis did not obliterate differences in chemical composition between calpionellids and other components.

Keywords: calpionellids, ultrastructure, Tithonian, Berriasian, micrite, carbonate diagenesis

Introduction

During the Late Jurassic, rock-forming calcareous microplankton, primarily consisting of calcareous dinoflagellates, chitinoidellids, and calpionellids, became a significant component of oceanic planktonic ecosystems (Bralower et al. 1989; Katz et al. 2004; Boughdiri et al. 2006; López-Martínez et al. 2013; Knoll & Follows 2016; Petrova et al. 2017; Vishnevskaya 2017; Kietzmann & Scasso 2020; Casellato & Erba 2021; Kietzmann et al. 2021, 2023). This increase in calpionellid abundance coincides with the rise in abundance of calcareous nannoplankton (especially nannoconids) during the Tithonian (Wieczorek 1988; Bornemann et al. 2003; Weissert & Erba 2004; Aubry et al. 2005; Tremolada et al. 2006; Casellato 2010). Together with high abundance of calcareous nannofossils, the high abundance of calcareous microplankton contributed to their rock-forming potential and to the deposition of pelagic oozes (the so-called biancone and maiolica facies) during the late Tithonian in the Tethys Ocean (Noël & Busson 1990; Busson & Noël 1991). The onset of pelagic ooze deposition is associated with a major evolutionary change in microplankton ultrastructure because the loricae of the genus *Chitinoidella* possess a microgranular layer (Ölveczká et al. 2024), whereas the loricae of *Praetintinnopsella*, *Crassicollaria* and *Calpionella* possess a hyaline layer (Aubry et al. 1975; Bolli 1980; Vincent et al. 1980; Remane 1985; Duchamp-Alphonse et al. 2009). The stratigraphic transition from the microgranular chitinoidells to hyaline calpionellids starts with the appearance of genera *Praetintinnopsella* in the *Praetintinnopsella* Zone and with the subsequent appearance of *Tintinnopsella, Crassicollaria* and *Calpionella* at the base of the *Crassicollaria* Zone in the higher part of the upper

✉ corresponding author: Diana Ölveczká
diana.olveczka@savba.sk

Tithonian. This transition generally coincides or occurs just immediately prior to the replacement of red nodular marls and limestones (Ammonitico Rosso facies) by white or light-gray non-nodular mudstones (maiolica and biancone facies, Lakova et al. 1999; Bernoulli & Jenkyns 2009; Lukeneder et al. 2010; Petrova et al. 2012, 2025; Grabowski et al. 2017, 2019; Benzaggagh 2021; Lodowski et al. 2024), near the boundary of the magnetochrons 19 and 20. This facies change is not only associated with the disappearance of calpionellids with microgranular loricae structure (Grandesso 1977; Lakova 1993; Reháková 2002; Michalík et al. 2009, 2016, 2021; Michalík & Reháková 2011; Wimbledon et al. 2020; Granier et al. 2023) but also with the so-called Nannofossil Calcification Event characterized by high abundance of heavily-calcified nannoliths (Bornemann et al. 2003; Tremolada et al. 2006). However, it remains unclear whether the hyaline walls of *Praetintinnopsella*, *Crassicollaria* and *Calpionella* differ from each other and whether they changed through time.

Earlier suggestions that *Praetintinnopsella* evolved from chitinoidellids were based on the assumption that its external layer exhibits a microgranular structure (Remane 1985). However, Ölveczká et al. (2024) demonstrated that (1) the test structure of *Praetintinnopsella* does not possess any microgranular layer and that its external layer consists only of an organic rim. Although the similarity in ultrastructure between chitinoidellids and *Praetintinnopsella* still requires further investigation, the difference in the ultrastructure of these two genera rather contradicts the idea that chitinoidellids and *Praetintinnopsella* represent a single phylogenetic lineage. Several studies documented the ultrastructure of *Calpionella*, *Tintinnopsella* or *Remaniella* (Aubry et al. 1975; Bolli 1980; Reháková & Michalík 1993). Aubry et al. (1975) showed that the test of the genera *Tintinnopsella* and *Calpionella* is composed of a single layer of small polyhedral, helicoidally-arranged crystals, with the smallest diameters equal to 0.3–0.4 μm and largest crystals attaining 5 μm in fine-grained limestones and marls of the Tunisian Dorsale (NE Tunisia). Reháková & Michalík (1993) showed that the rhombohedral or scalenohedral crystals of the hyaline layer of the genus *Calpionella* from the Tithonian–Berriasian deposits in the Western Carpathians tend to be larger (4–7 μm in length) and are oriented perpendicularly to the inner lorica surface in *Calpionella*. However, the ultrastructure of the hyaline layer in *Praetintinnopsella* and *Crassicollaria*, as well as their susceptibility to diagenetic modification, remains undocumented, obfuscating the phylogenetic relationship between them (Remane 1964, 1998; Vincent et al. 1980; Reháková & Michalík 1993; Fözy et al. 2011; Benzaggagh 2020, 2021).

In this study, we examine the microtexture of calpionellid-rich pelagic limestones (maiolica and biancone facies) and assess the preservation and ultrastructure of the hyaline layer in the genera *Praetintinnopsella*, *Crassicollaria* and *Calpionella* from the Pieniny Klippen Belt (Western Carpathians), using scanning electron microscopy (SEM), backscattered electron imaging (BSE), and wavelength-dispersive spectroscopy (WDS). We focus on the stratigraphic transition from hyaline loricae of the genus *Praetintinnopsella* to the loricae of the genus *Calpionella*. As the Upper Jurassic and Lower Cretaceous pelagic deposits in the Tethyan realm are lithified and have undergone varying degrees of cementation, dissolution and recrystallization, we also assess the diagenetic phases that affected the overall sediment microtexture and modified the original test ultrastructure (Remane 1963). Such analyses can provide valuable insights into the potential use of calpionellid geochemical signatures (e.g., Mg/Ca ratio) or isotopic proxies as tracers of past changes in temperature and other environmental variables (Žák et al. 2011). Therefore, our aims are: (1) to compare the ultrastructure of the hyaline layer among *Praetintinnopsella, Crassicollaria* and *Calpionella,* (2) to evaluate the preservation of microtexture of the micritic sediments that embed calpionellids, and (3) to assess the degree of diagenetic modification of the hyaline layer by examining its preservation under SEM and by comparing the chemical composition of the tests with that of adjacent micritic grains (representing a mixture of well-preserved or neomorphosed nannofossils and micritic cements) based on BSE and WDS.

Material and methods

Stratigraphic sections

Sixty-three thin-section samples used in SEM, BSE and WDS analyses of the ultrastructure and preservation of *Praetintinnopsella*, *Crassicollaria*, and *Calpionella* were collected from upper Tithonian and lower Berriasian deposits of three sections in the Pieniny Klippen Belt (PKB) of the Western Carpathians. They include Brodno and Snežnica sections belonging to the deep-water Kysuca–Pieniny Succession (Michalík et al. 2009, 2021) and the Strapková section belonging to the Orava Succession (Fig. 1, Schlögl et al. 2000; Michalík et al. 2016). The Jurassic facies succession comprising the Allgäu and Adnet formations at Strapková section is very similar to those of the Fatric Unit (Central Western Carpathians). This succession may in fact represent a segment of the frontal nappes of the Fatric Unit that was initially not located in the depositional area of the PKB and was emplaced into the PKB accretionary wedge formed by the Oravic units during the Late Cretaceous or later (e.g., Plašienka 2019). All three sections record the transition from the lower Tithonian part of the Czorsztyn Limestone Formation to the upper Tithonian–lowermost Berriasian Pieniny Limestone Formation (Michalík et al. 1990, 2009, 2019, 2021; Houša et al. 1996, 1999; Michalík & Reháková 2011). *Praetintinnopsella* occurs in the uppermost part of the Czorsztyn Limestone Formation and *Crassicollaria* and *Calpionella* co-occur in the lowermost part of the Pieniny Limestone Formation at all three sections.

Brodno section is located north of Žilina in northwestern Slovakia (49°16’02.16”N, 18°45’12.16”E), in an abandoned quarry within the valley of Kysuca river. The section is

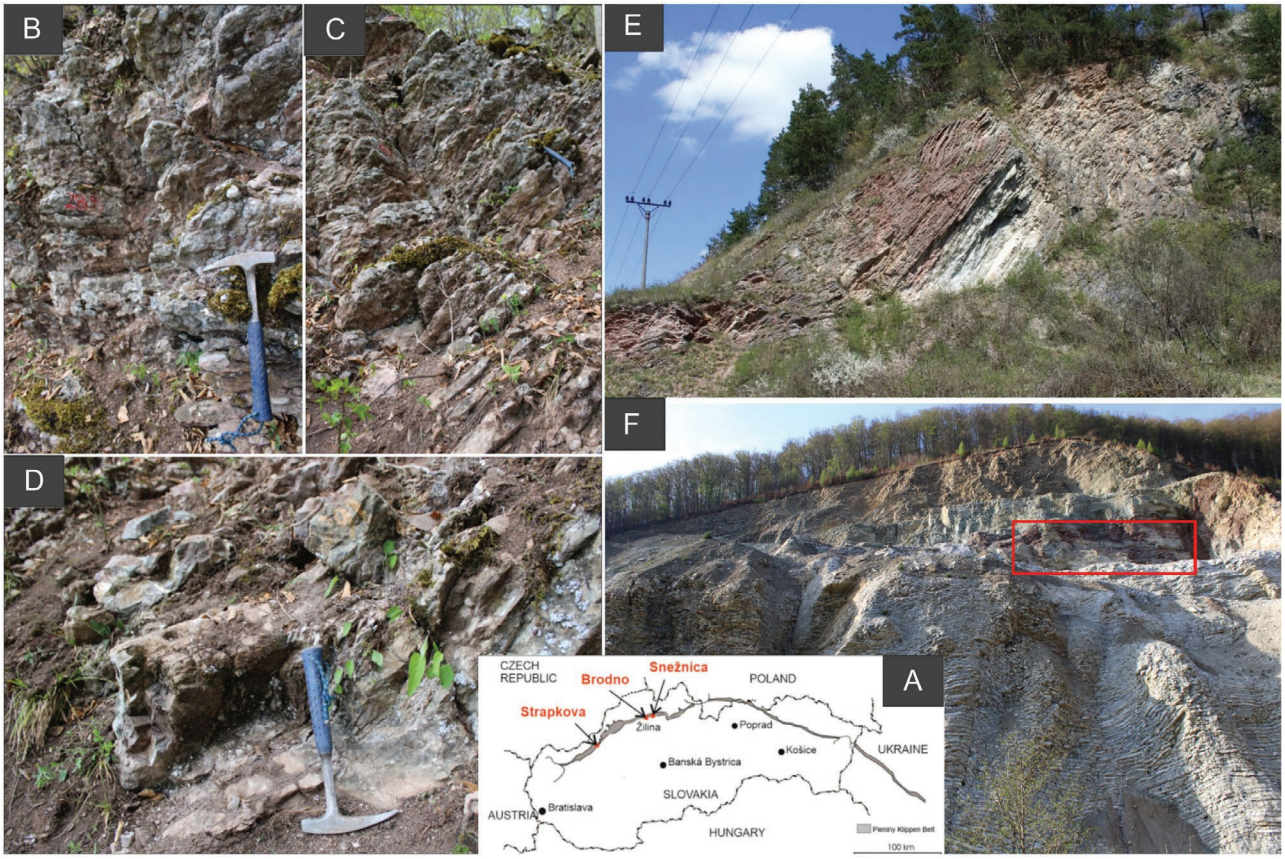

Fig. 1. (A) Geographic location of Brodno, Snežnica and Strapková sections in the Pieniny Klippen Belt (Western Carpathians) in Slovakia. **(B–D)** Pink cherty "Ammonotico Rosso" limestones of the Czorsztyn Limestone Formation at the Strapková section. **(E, F)** Nodular red "Ammonitico Rosso" limestones of the Czorsztyn Limestone Formation overlain by grayish micritic limestones of the Pieniny Limestone Formation at the Brodno and Snežnica quarry (red rectangle depicts the investigated section).

approximately 25 m thick and represents typical eupelagic sedimentation within the Pieniny Klippen Belt (Michalík et al. 1990, 2009; Reháková & Michalík 1992; Kowal-Kasprzyk & Reháková 2019). The base of the section is composed of red and pink, thick-bedded, nodular limestones (Ammonitico Rosso) of the Czorsztyn Limestone Formation, characterized by the *Saccocoma–Globochaete* microfacies. This formation is overlain by light-gray, thin-bedded, non-nodular micritic limestones of the Pieniny Limestone Formation, containing calpionellid–*Globochaete*–radiolarian microfacies. Our sampling targeted the uppermost Tithonian part of the Czorsztyn Limestone Formation (corresponding to the *Praetintinnopsella* Zone) and the lowermost Berriasian part of the Pieniny Limestone Formation (corresponding to the *Crassicollaria* and *Calpionella* zones). *Praetintinnopsella andrusovi* co-occurs with *Chitinoidella boneti*, *Dobeniella cubensis*, and *Semichitinoidella* sp. in the *Praetintinnopsella* Zone (beds 94–98, bed numbers according to Michalík et al. 2009) and with *Crassicollaria* in the *Remanei* Subzone (bed 98–99) in the upper part of the Czorsztyn Limestone Formation. The *Intermedia* Subzone (beds 6–17) is characterized by the appearance of *Calpionella grandalpina* and by the presence of abundant small *Crassicollaria brevis,* co-occurring with *Calpionella alpina, Crassicollaria parvula*, and *Tintinnopsella carpathica*. In the *Colomi* Subzone (beds 18–23D), *Crassicollaria parvula* and *Crassicollaria colomi* are common alongside *Calpionella grandalpina* and *Calpionella alpina.* The *Alpina* Subzone (beds 24A–27C) is dominated by *Calpionella alpina* and *Calpionella grandalpina*, whereas *Crassicollaria parvula* and *Tintinnopsella carpathica* are less common.

Snežnica section is located in an abandoned quarry ~1.5 km eastward from Brodno, near the road leading to the village Snežnica in northwestern Slovakia (49°16'14.35"N, 18°46'31.18"E, Michalík et al. 2019). The base of the section sampled here is composed of gray and red, thick-bedded nodular limestones (Ammonitico Rosso) of the Czorsztyn Limestone Formation with stratiform cherts and well-sorted calciturbiditic layers, with wackestones to packstones rich in *Saccoccoma*, globochaetes and chitinoidellids. This formation is overlain by gray, thin-bedded, non-nodular, micritic limestones of the Pieniny Limestone Formation (*Remanei* Subzone). *Praetintinnopsella andrusovi* is rare and co-occurs with chitinoidellids in the *Praetintinnopsella* Zone. In the *Remanei* Subzone of the standard *Crassicollaria* Zone, *Crassicollaria parvula*, *Crassicollaria massutiniana*, and *Tintinnopsella remanei* are most common, co-occurring and *Calpionella alpina*.

Strapková section is located northeast of the Vršatecké Podhradie village in northwestern Slovakia (49°04'09.34"N, 18°10'00.85"E), on the slope of Strapková hill (Schlögl et al. 2000; Michalík et al. 2016). A 12 m-thick succession sampled in this study exposes eight meters of reddish, thin-bedded, nodular to poorly-nodular limestones of the Czorsztyn Limestone Formation (with the cyst *Pulla*, *Malmica* and the calpionellid *Chitinoidella* zones), including *Saccoccoma* packstones, *Saccocoma–Globochaete*–radiolarian packstones, and *Saccocoma–Globochaete* wackstones and packstones, overlain by four meters of the Pieniny Limestone Formation. The transition between the Czorsztyn and Pieniny formations is represented by a ~1 m-thick interval with reddish to grayish, weakly-nodular to non-nodular limestones with *Praetintinnopsella*, passing upward into light-gray, thin-bedded mudstones of the Pieniny Limestone Formation (*Crassicollaria* and *Calpionella* zones). Our sampling targeted the lowermost part of upper Tithonian Czorsztyn Limestone Formation (corresponding to the *Praetintinnopsella* Zone) and the upper Tithonian part of the Pieniny Limestone Formation (corresponding to the *Crassicollaria* Zone). The first *Semichitinoidella* sp. appearing in the *Dobeni* Subzone (bed at 288.23 m, stratigraphic position according to Michalík et al. 2016). *Praetintinnopsella andrusovi* co-occurs with rare *Chitinoidella boneti* and cysts of *Colomisphaera carpathica* in the *Praetintinnopsella* Zone (beds 291–292).

Analyses

All samples and thin-sections are archived at the Institute of Earth Sciences of the Slovak Academy of Sciences in Bratislava. Calpionellids were identified to genus and species level with a light microscope (LM) Axio ZEISS Scope A1. For analyses of test ultrastructure, we selected only specimens identified to species level (*Praetintinnopsella andrusovi*, *Tintinnopsella remanei*, *Crassicollaria parvula, Crassicollaria massutiniana, Crassicollaria intermedia, Crassicollaria brevis*, *Calpionella alpina* and *Calpionella grandalpina*). As crystal size and shape can depend on the orientation of specimens with respect to the thin-section plane, we only assess longitudinal sections in SEM analyses of size and shape of crystals in the loricae. The positions of the loricae selected for ultrastructural study were marked on the polished, uncovered thin-sections under a light microscope. Although we have attempted to photograph the same individuals with all three methods (LM, SEM, BSE), this approach was not always possible owing to the fact that the specimens in optical microscope are visible across the entire thickness of thin-sections whereas they can be observed just on the uppermost surface of thin sections in the BSE and SEM.

The length and width of identifiable specimens of three genera (*Praetintinnopsella, Crassicollaria, Calpionella*) and of crystals forming their hyaline layers were measured using SEM at magnification of 500–5000× (JEOL JSM-6390LV), as differences in chemical composition among crystals and adjacent micritic grains are often poorly visible in BSE images. Thin sections were cleaned, treated with 3 % acetic acid for about 3–5 seconds, and coated with gold for SEM analyses. In total, 1038 measurements of crystal size were obtained (*Praetintinnopsella* = 458 specimens, *Crassicollaria* = 270 specimens, *Calpionella* = 310 specimens). Regardless of the orientation of the crystals relative to the inner test surface, the crystal length in the hyaline layer corresponds to the maximum dimension along the longer axis, while their width corresponds to the maximum dimension perpendicular to it. The ultrastructure data are available in Electronic Supplement S1, and R language scripts (R Core Team 2024) are available in the Electronic Supplement S2.

Sixty-three polished thin-sections (each thin section corresponds to a unique sampling level) from Brodno (n = 38), Strapková (n = 14) and Snežnica (n = 11) were coated with platinum to assess the chemical composition of loricae, micritic grains located outside of loricae, and void-filling microsparite with microprobe microanalyzer (EMPA), using BSE and WDS. Elemental concentrations of Mg, S, Sr, Mn, and Fe were measured at 15 kV and 16 nA, with the spot beam diameter of 5–7 μm (and to 1 μm for semiquantitative element maps). Detection limits under these conditions are ~110 ppm for Mg, ~170 ppm for S, ~220 ppm for Sr, ~150 ppm for Mn, and ~134 ppm for Fe. Within each thin-section, the chemical composition of four calpionellid individuals was measured. For each individual, two spots were selected on the lorica wall (and, if the thickness of the wall allowed, one measurement was from the collar), one spot in the interior of the specimen (typically filled by microspar), and one spot in the adjacent micritic grains (formed by well-preserved or neomorphosed nannofossil remains and micritic cements). Median concentrations of elements were computed for loricae, internal infills. and external micritic grains, both separately for each genus (across all sections) and for each section (across all genera), and visualized in boxplots. In addition, we evaluated whether median per-sample element concentrations in loricae correlate

Fig. 2. Microtexture of pelagic mudstones and wackestones of the Czorszstyn (A, B) and Pieniny Limestone formations (C–H) in SEM. **(A, B)** Nannofossil sections (arrows) separated by coarser, cement-representing microspar at Strapková (A – 28.4 m, B – 290.55 m). Scale: 5 μm. **(C, D)** The sediment formed by dispersed remains of relatively complete, dissolution-resistant nannofossils (dark gray), by identifiable micritic grains (<5 μm) and by larger microspar that rims larger bioclasts or fills the interior of the test of *Calpionella alpina* (white), and by microplankton remains (light gray). Black – authigenic quartz (Brodno, bed 15B). Scales: 10 μm. **(E, F)** Details of E, F at Brodno (bed 15B), with sections of nannofossils. Scales: 5 μm. **(G, H)** Microspar filling the interior of *Crassicollaria* lorica (dashed line), locally embedding relicts of nannofossils (nan), and micritic particles with dispersed nannofossils in the matrix adjacent to the test, with some micritic grains gradually passing into or engulfing nannofossils, without any clear intercrystalline boundaries. Brodno bed 1A (base). Abbreviations: Chi – *Chitinoidella*; Cras – *Crassicollaria*; nan – nannofossils; qtz – quartz; mic – micrite; mspar – microspar. Scales: 5 μm.

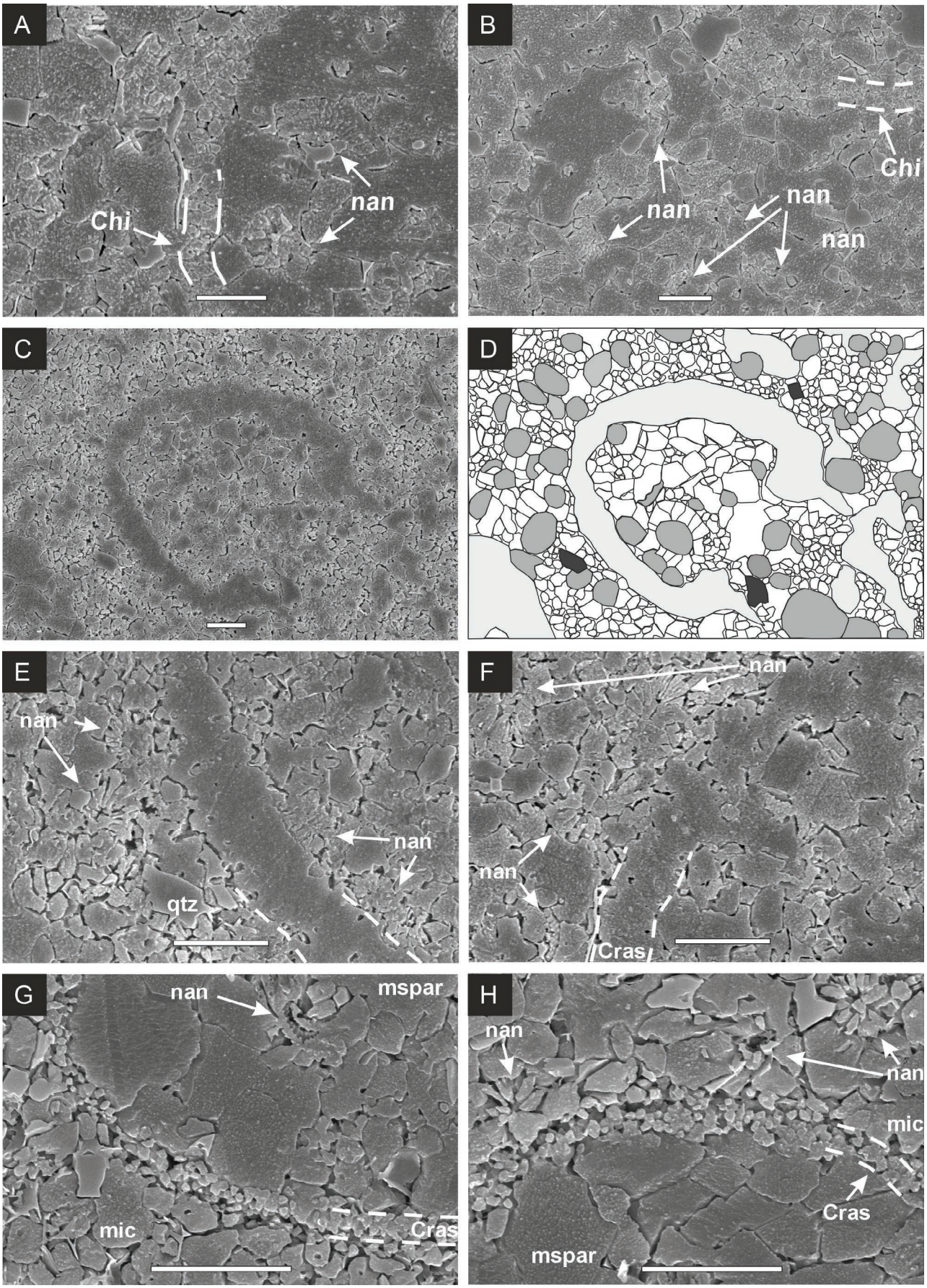
A
Chi
nan
B
Chi
nan
nan
nan
C
D
E
nan
nan
qtz
F
nan
nan
Cras
G
nan
mspar
mic
Cras
H
nan
nan
mic
Cras
mspar

with median per-sample element concentrations in internal infills and external micrite. The elemental concentrations are available in Electronic Supplement S3, and R language scripts are available in the Electronic Supplement S4.

Results

Microtexture

The microtexture of pelagic mudstones and wackestones of the Czorsztyn and Pieniny Limestone formations is characterized by clustered or fitted fabric (sensu Kaczmarek et al. 2015) and meshed or coalescent microtexture (sensu Saïag et al. 2019). It includes subhedral to euhedral micritic crystals (Fig. 2A, B), local microsparite patches, micrite or microsparite filling intra- or interskeletal voids, nannofossil remains (Fig. 2C, D), and larger microplankton remains, such as calcareous dinocysts, calpionellids, globochaetes, and *Saccoccoma*. Nannofossils are either represented by identifiable and well-demarcated complete nannoliths (mainly *Conusphaera* and *Nannolithus*) and coccoliths (mainly *Watznaueria*), which reach ~5–8 um in size, or by nannofossil fragments embedded in larger micritic crystals or in microsparitic void-filling cement (Figs. 2E–H, 3A–D). The interlocking subhedral to euhedral micritic crystals that are ~2–4 μm long typically exhibit straight and curvilinear surfaces (Fig. 3E, F), although some crystals also show irregular (knobby) surfaces. Small, non-identifiable euhedral crystals, 1–5 μm in size, locally resemble fragments of nannoliths and coccoliths (or crystals forming the external layer in calcareous dinocysts). However, such crystals also frequently fill small pores among nannofossils and other grains and probably frequently represent micritic cements.

SEM images show that larger microsparitic crystals attached to the walls of calpionellid tests or filling them are relatively smooth, in contrast to more irregular surfaces of micritic crystals that occur among tests (Fig. 2G, H). Some calpionellid loricae exhibit marked variability in thickness, with localized thinning or thickening induced by cement overgrowths, not significantly protruding beyond the internal or external lorica surface (Fig. 2C, D). In some specimens, the boundaries between individual crystals within the hyaline layer can be blurred by crystal amalgamation (in Fig. 3E, F) and the inter-crystalline boundaries between epitaxial, micritic or microsparitic cements and nannofossils are locally indistinct (Fig. 2G, H). Nannofossil fragments or non-identifiable grains may also be embedded within larger crystals, reflecting aggrading neomorphism. Authigenic quartz and albite are dispersed in the matrix as euhedral crystals while microdolomite crystals (<10 μm) occur within crinoid ossicles and in syntaxial rims enveloping *Saccocoma* ossicles (Fig. 3G, H). We note that isopachous fringing crusts formed by calcite prisms or fibers (as observed in *Schizosphaerella* in the Jurassic hemipelagic Tethyan deposits, Kälin & Bernoulli 1984; Erba et al. 2019) do not develop on the tests of hyaline calpionellids or nannofossils in the Pieniny Limestone Formation, although the external prismatic layer can be observed in some cadosinids (*Cadosina semiradiata,* e.g., Reháková & Michalík 1996) or in *Semichitinoidella* (Nowak 1978; Ölveczká et al. 2024) in the Czorsztyn Limestone Formation.

Praetintinnopsella ultrastructure and composition

The loricae of *Praetintinnopsella* reach 34–56 μm in length (median=46 μm) and 34–47 μm in width (median=41 μm). They are composed of a hyaline layer which is surrounded by a dark, irregularly-thick organic, amorphous rim or lining, or the top of the hyaline layer is separated from the adjacent sediment by a ~1 μm thick cavity (Fig. 4). Although this ~1 μm-thick layer resembles a microgranular layer under a light microscope, BSE and SEM analyses show that it contains no calcitic material. The mean thickness of hyaline layer is ~1.90–2.0 μm. Crystals within the hyaline layer are densely packed, subhedral to anhedral, and arranged in one or two rows. They are relatively equidimensional or slightly elongated, with a median length equal to 1.1 μm, median width equal to 0.81 μm, and median length/width ratio equal to 1.35 (Fig. 5).

The elemental maps reveal that the hyaline layer is brighter relative to the matrix-forming low-Mg calcite crystals (micritic or microsparitic crystals that correspond to fragments of nannofossils or to cement that fills interspaces), with the brightest grains corresponding to small clay minerals (Fig. 6). The concentration of Mg is slightly reduced, and the concentration of S is elevated near the external boundary where the external rim is located (Fig. 6D). Median Mg concentrations in the loricae of *Praetintinnopsella* (median=3550 ppm) are higher than those in the micritic crystals adjacent to loricae (median=3070 ppm, Fig. 7) and in the infill of their tests (median=3040 ppm). In contrast, Mn concentrations in the loricae of

Fig. 3. Microtexture of pelagic mudstones and wackestones of the Czorszstyn and Pieniny Limestone formations in BSE, with dashed lines marking the contours of the hyaline walls of calpionellids. **(A, B)** Fragments of watznaueriacean coccoliths (white arrows) among micritic grains (A) or engulfed by void-filling microspar inside a calcareous dinoflagellate cyst (B) at Brodno (bed 1A). **(C, D)** Interspaces among nannofossils (large white arrows) are typically filled by 1–5 μm euhedral micritic crystals with sharp surfaces (small white arrows) at Brodno (bed 27E). Some nannofossils are partly recrystallized due to aggrading neomorphism (outline delimited by a gray dashed contour line in D). Individual plates or fragments of nannoliths also possess sharp surfaces. **(E)** Authigenic quartz, albite and dolomite in the Pieniny Limestone Formation at Brodno (bed 8A). **(F)** Microdolomite in a crinoid ossicle in the Pieniny Limestone Formation at Brodno (bed 27E). **(G)** High frequency of authigenic quartz (dark gray colour) in the Czorsztyn Limestone Formation at Strapková 288.3 m. The outline of the calpionellid lorica, weakly demarcated from a similarly bright infill, is marked by dark gray dashed lines. **(H)** High frequency of authigenic quartz in the Pieniny Formation at Strapková 292.8 m. Abbreviations: qtz – quartz; alb – albite; dol – dolomite. Scales: 10 μm.

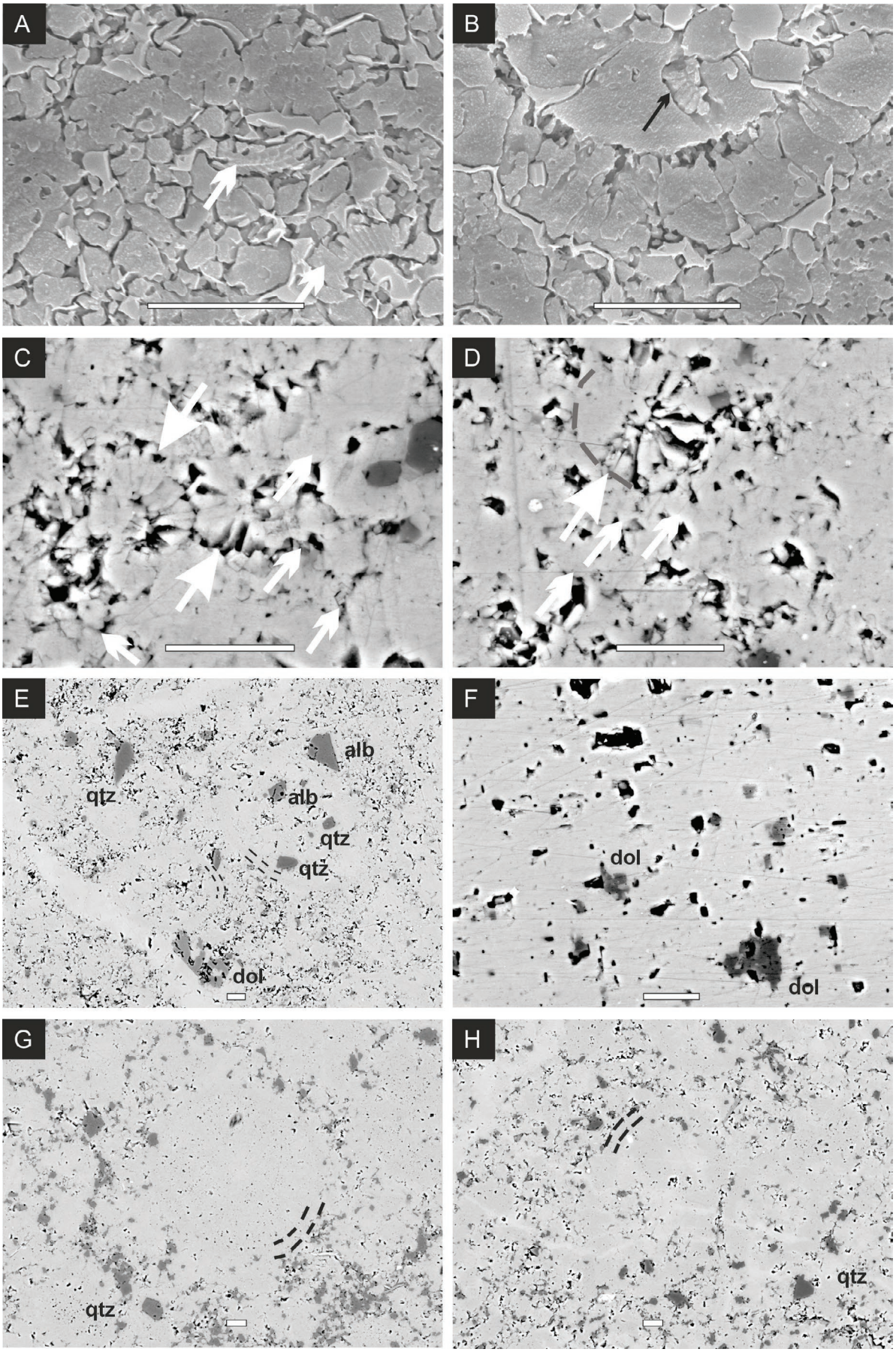
A
B
C
D
E
alb
qtz
alb
qtz
qtz
dol
F
dol
dol
G
qtz
H
qtz

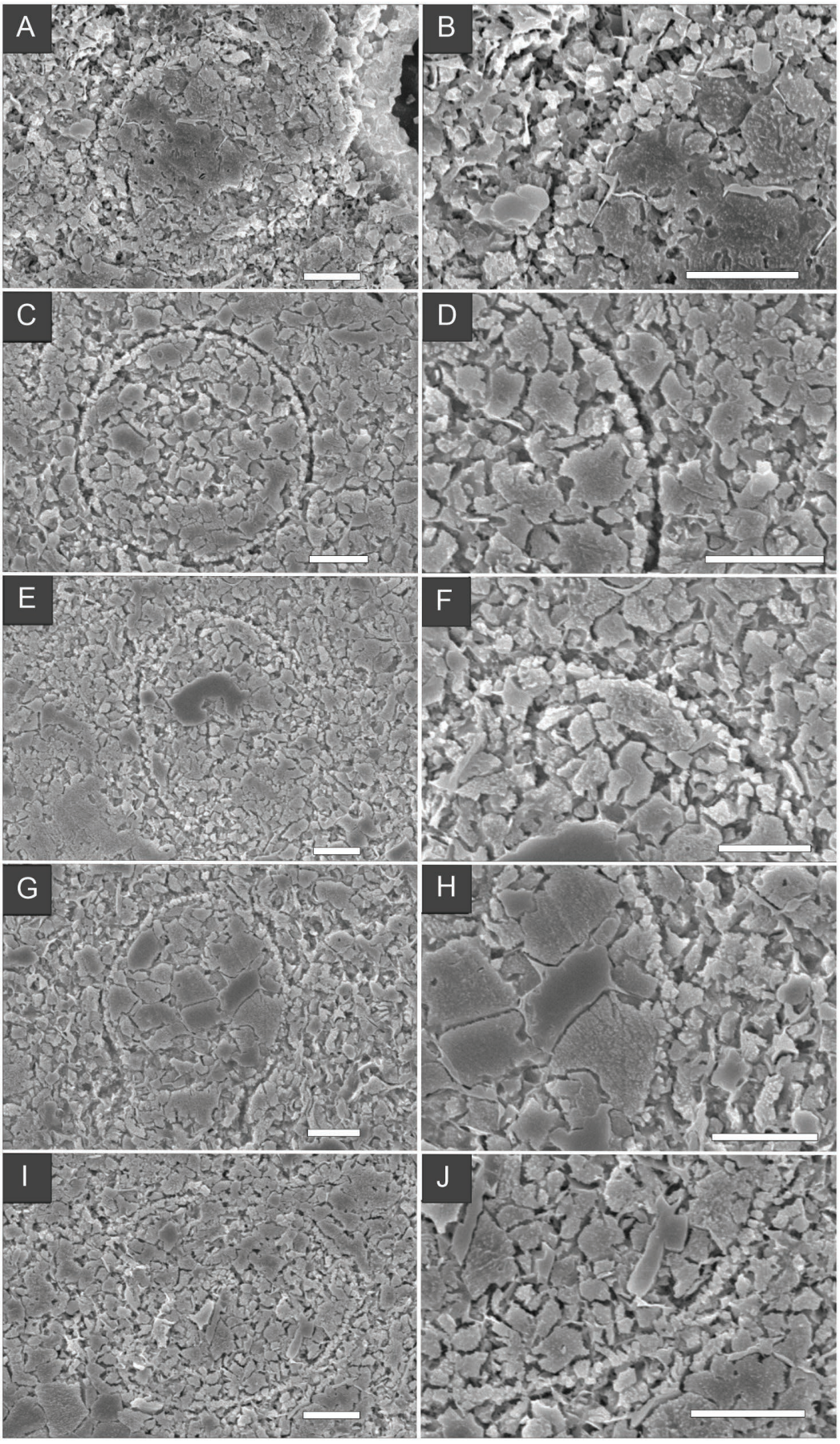
A
B
C
D
E
F
G
H
I
J

Fig. 4. Ultrastructure of *Praetintinnopsella* with the internal hyaline layer and dark external rim in five specimens under SEM. **(A, B)** Bed 96 upper part at Brodno, *Praetintinnopsella* Zone, Sp. 5. **(C, D)** Bed Sn 19.21 (Snežnica, *Praetintinnopsella* Zone). **(E, F)** Bed Sn 19.21 (Snežnica, *Praetintinnopsella* Zone). **(G, H)** Bed Sn 19.21 (Snežnica, *Praetintinnopsella* Zone). **(I, J)** Bed Sn 19.24 (Snežnica, Remanei Subzone). Scale=10 μm in SEM.

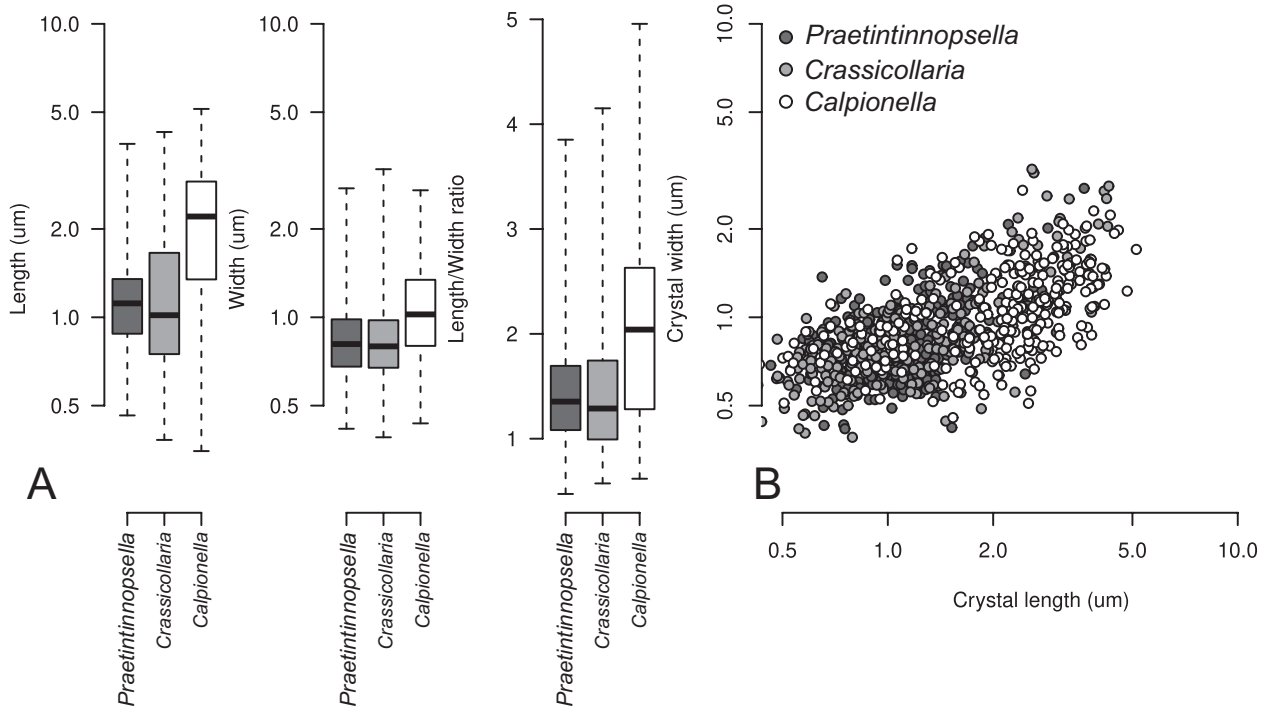

Fig. 5. (A) Boxplots with the length and width of crystals that constitute the hyaline layer, and the length/width ratio in *Praetintinnopsella*, *Crassicollaria* and *Calpionella*. Median crystal length and width is smaller in *Praetintinnopsella* and *Crassicollaria* than in *Calpionella*. *Calpionella* exhibits the highest length/width ratios, i.e., its crystals are more elongated than in other two genera. The variability (the extent of the boxes corresponding to the inter-quartile range, IQR) in length, width and length/width ratio is somewhat larger in *Calpionella*. **(B)** The relation between length and width of lorica-forming crystals, separating longer and broader crystals of *Calpionella* from shorter and narrower crystals of *Praetintinnopsella* and *Crassicollaria*.

Praetintinnopsella (median=280 ppm) are lower than in the micritic crystals (median=300 ppm) and in the infill of their tests (median=460 ppm). Sr concentrations are extremely low (typically below the detection limit) in loricae (median=9 ppm), and slightly higher in the micritic crystals (median=85 ppm) and in the lorica infills (median=190 ppm). S concentrations are also very low, and the difference between the loricae and the adjacent sediment is not resolved by WDS analyses in loricae (median content in loricae=110 ppm, median content of micritic crystals=120 ppm, and median content of infills =92 ppm).

Crassicollaria ultrastructure and composition

The loricae of *Crassicollaria* range from 65 to 81 μm in length (median=69 μm) and 33–52 μm in width (median =46 μm). The mean thickness of the hyaline layer varies between 2.76–3.84 μm. It is composed of very thin, small (median length=1 μm, median width=0.8, median length/width ratio =1.29), euhedral, densely-packed, relatively equidimensional crystals that are slightly longer than wider (Fig. 8). The preservation of crystals within the hyaline layer varies significantly among specimens from the same bed and across different localities, leading to differences in crystals packing, shape, and size (with some loricae exhibiting amalgamation of crystals). Relatively well-preserved specimens from Brodno and Snežnica display a hyaline layer that is composed of interconnected, slightly elongated, densely packed plates (Fig. 8). In contrast, the crystals forming the hyaline layer at Strapková are poorly defined due to the loss of inter-crystalline boundaries and recrystallization (aggrading neomorphism) (Fig. 8). In some beds (Sn 19.24, BR 98 up and ST 291,32), the crystals within the hyaline layer are smaller, more equidimensional than elongated, and locally arranged in two rows, similar to the hyaline layer of *Praetintinnopsella* (Fig. 8).

High-resolution elemental maps show that the hyaline layer is markedly enriched in Mg and in S (Figs. 9, 10), in contrast to the composition of the internal infill and the adjacent micritic matrix that is on average poorer in Mg. Void-filling cements are also poor in Mg. Median Mg concentrations in loricae of

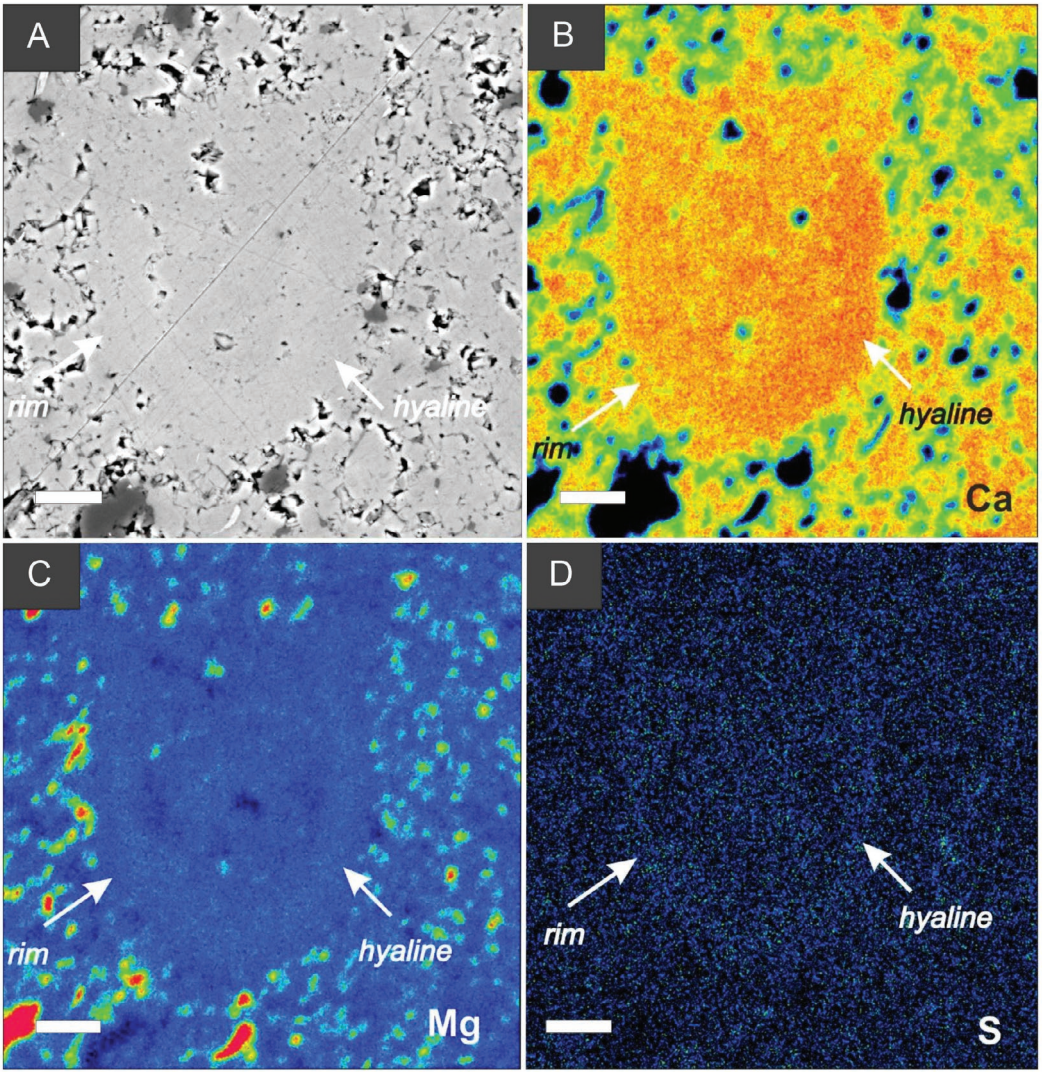

Fig. 6. BSE and the corresponding electron microprobe maps showing that the internal hyaline layer of *Praetintinnopsella* is enriched in magnesium (Mg) and sulphur (S) relative to the external matrix and internal filling, as confirmed by quantitative WDS measurements. **(A–D)** The lorica of *Praetintinnopsella* with the collar with internal hyaline layer and external dark organic rim. Snežnica (bed 19.21). The change from blue to red colours corresponds to an increase in the concentration of each element (Ca, Mg and S). Scale=10 µm.

Crassicollaria (median=3560 ppm) exceed those in the micritic crystals adjacent to loricae (median=3300 ppm) and in the infill of their tests (median=3120 ppm, Fig. 7). In contrast, Mn concentrations are two times lower in loricae (median =290 ppm) than in the micritic crystals adjacent to loricae (median=420 ppm) and in the infill of their tests (median =470 ppm). Concentrations of Sr (<200 ppm) and S (<175 ppm) are invariably very low.

Calpionella ultrastructure and composition

The loricae of *Calpionella* specimens range from 40 to 75 µm in length (median=55 µm) and 37–71 µm in width (median=46 µm). The thickness of the hyaline layer varies between 5.1–5.2 um. SEM images reveal that the hyaline wall is composed of slender prismatic crystals (length/width ratio is ~2) oriented perpendicularly or obliquely to the inner surface of the lorica wall in longitudinal sections (Figs. 11, 12), although the apparent shape of crystals depends on the orientation of the sections relative to the crystal growth direction. The prisms appear as sharp-edged and elongated crystals (median length=2.2 µm, median width=1.02 µm). Some specimens exhibit two distinct layers or sheets (Fig. 12) that may reflect imbrication or shingle-like arrangement of these layers in longitudinal sections as observed by Aubry et al. (1975). No differences were observed in the shape of the crystals in transversal and longitudinal sections of the loricae. The crystals are rather irregular and anhedral at Snežnica and Strapková whereas they are more elongated, densely-packed and subhedral at Brodno (Fig. 11).

Similarly to *Crassicollaria*, high-resolution maps demonstrate that the walls of *Calpionella* specimens, in comparison

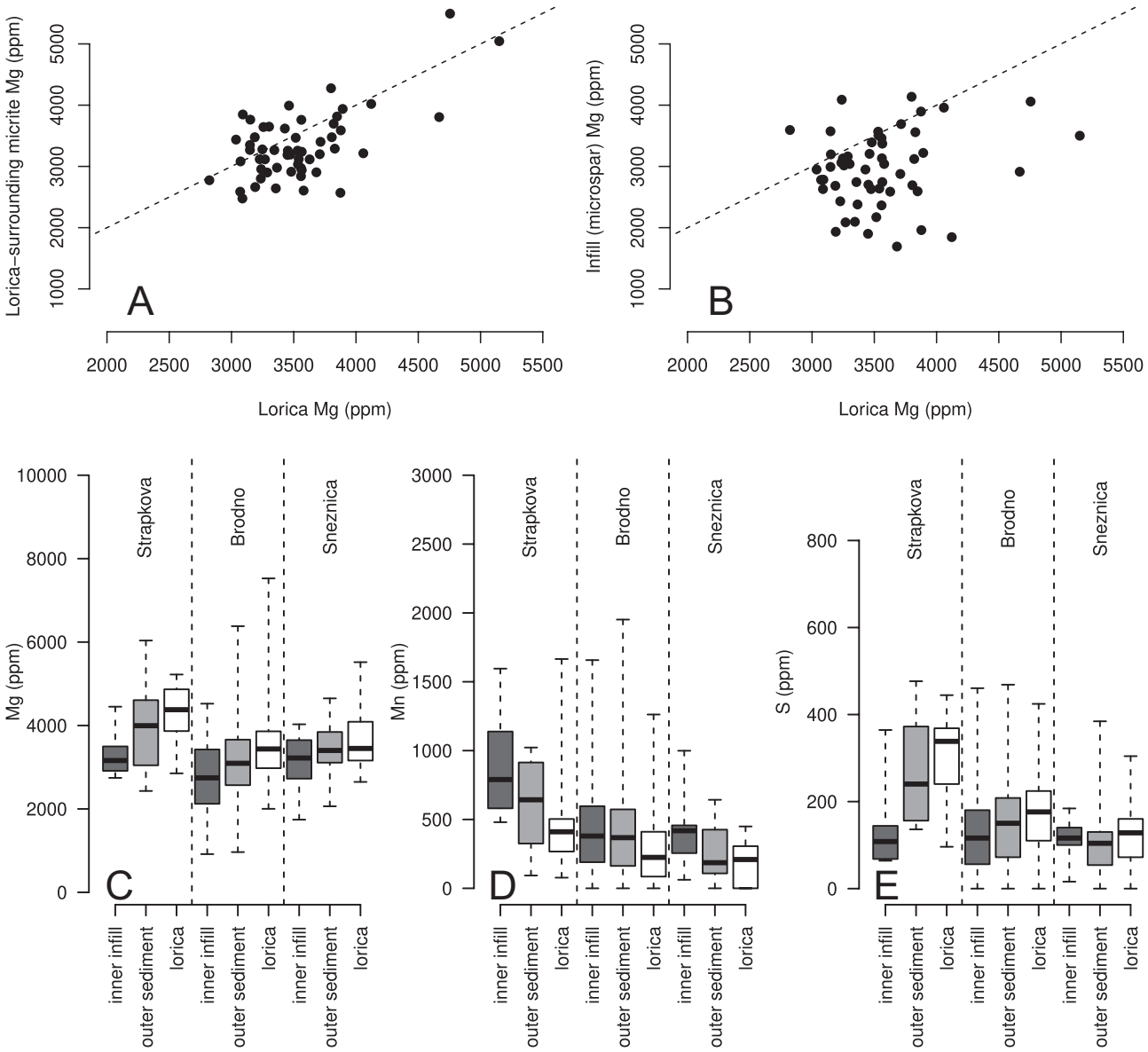

Fig. 7. (A, B) The median per-sample concentrations of Mg observed in micritic grains correlate positively with median per-sample concentrations of Mg in loricae of three genera (A). In contrast, median per-sample concentration of Mg observed in test (microspar) infills does not correlate with median per-sample concentration of Mg in loricae (B). **(C–E)** Differences in geochemical composition between sediment (enriched in Mn) and loricae of calpionellids (*Praetintinnopsella*, *Crassicollaria* and *Calpionella*). The loricae are depleted in Mn and enriched in S and Mg relative to the composition of sediment matrix and lorica infill. The Sr concentrations do not differ between the loricae and sediment matrix, indicating that the mud is not derived from recrystallized aragonitic elements.

with the adjacent and internal micrite, exhibit high brightness and are enriched in Mg (Fig. 13). These observations are supported by WDS analyses. Median Mg concentrations in *Calpionella* loricae (median=3420 ppm) exceed those in the micrite adjacent to loricae (median=3160 ppm) and in the infill of their tests (median=3010 ppm, Fig. 7). Median Mn concentrations in loricae (median=210 ppm) are lower than in the adjacent micrite (median=390 ppm) and in the infill of their tests (median=370 ppm). Sr concentrations are similarly low in loricae (median=194 ppm) and in the external micrite (median=203 ppm) and slightly higher in the lorica infills (median=300 ppm). Median S concentrations in loricae (median=170 ppm) are slightly higher in loricae than in the surrounding micrite (median=140 ppm) and in the infill of their tests (median=110 ppm).

Between-section differences in the preservation and chemical composition of calpionellid loricae

Although Mg concentrations are higher in loricae than in lorica infills or in surrounding micrite, median per-sample Mg concentrations observed in micrite correlate positively with those

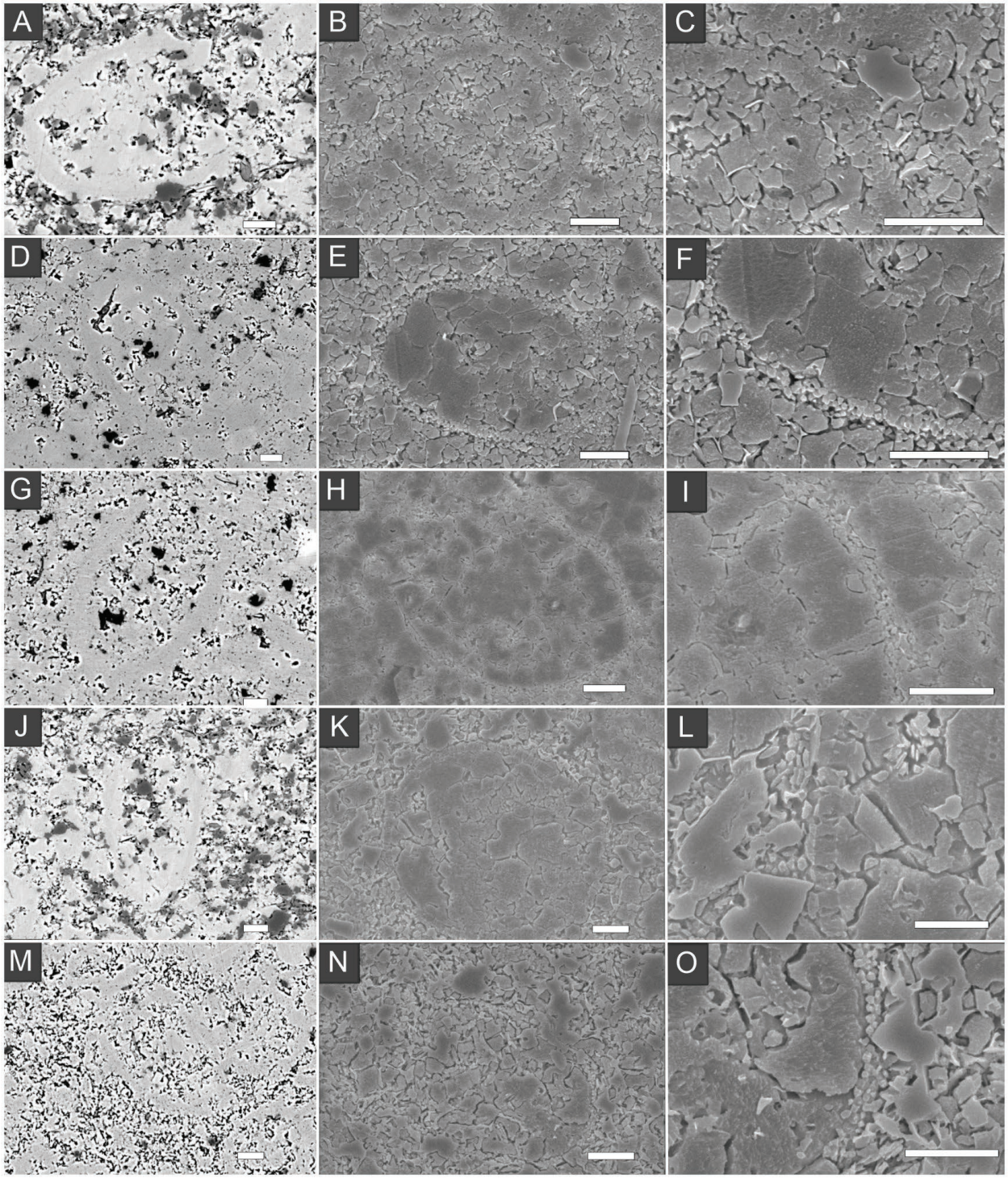

Fig. 8. Ultrastructure of *Crassicollaria* with the hyaline layer in specimens photographed with BSE (left column) and SEM (middle and right column). **(A)** Bed BR 10 upper part (Brodno, *Intermedia* Subzone). **(B, C)** Bed BR 1A base (Brodno, *Remanei* Subzone). **(D)** Bed Sn 19.25 middle (Snežnica, *Remanei* Subzone). **(E, F)** Bed BR 1A base (Brodno, *Remanei* Subzone). **(G)** Bed ST 291,45 (Strapková, *Remanei* Subzone). **(H, I)** Bed Sn 19.25 (Snežnica, *Remanei* Subzone). **(J)** Bed BR 2D up, Sp. 1. **(K, L)** Bed ST 291,32 (Strapková, *Remanei* Subzone). **(M)** Bed BR 10 (Brodno, *Intermedia* Subzone). **(N, O)** Bed ST 291,32 (Strapková, *Remanei* Subzone). Scale=10 µm.

measured in loricae (Spearman r=0.35, p=0.008, Fig. 7A). Thus, the stratigraphic and between-section variability in Mg concentrations within loricae is to some degree reflected by the micrite that surrounds them. This pattern is also observed for sulphur (Spearman r=0.3, p=0.025), strontium (Spearman r=0.38, p=0.005) and manganese (Spearman r=0.31, p=0.02). In contrast, median per-sample Mg concentration observed in test (microspar) infills does not correlate with Mg concen-

tration in the loricae (Spearman r=0.13, p=0.33, Fig. 7B), and a similar lack of correlation between microspar infills and loricae is observed for sulphur (Spearman r=−0.04, p=0.75), strontium (Spearman r=0.18, p=0.18) and manganese (Spearman r=0.18, p=0.19).

The chemical composition of micrite and internal cements differs between Brodno and Snežnica, on one hand, and Strapková, on the other hand (Fig. 7C–E). Mg concentrations in micritic crystals (median=640 ppm) and in test infills (median=790 ppm) are highest at Strapková and lowest at Brodno (median=370 ppm in micrite and 380 ppm in infills) and at Snežnica (median=190 ppm in micrite and 420 ppm in infills). Similarly, Fe concentrations in micrite (median=630 ppm) and in test infills (median=1880 ppm) are higher at Strapková than at Brodno (median=580 ppm in micrite and 560 ppm in infills) and at Snežnica (500 ppm in micrite and 410 ppm in infills). These differences are paralleled by higher Mn content of loricae at Strapková (median=410 ppm) than at Brodno (median=220 ppm) and Snežnica (median=210 ppm), and by higher Fe content of loricae at Strapková (median=860 ppm) than at Brodno (median=330 ppm), although Fe content is also high at Snežnica (median=910 ppm). Mg concentrations are higher at Strapková (Mg: 4000 ppm in micrite and 3160 ppm in infills) than at Brodno (Mg: 3090 ppm in micrite and 2740 ppm in infills) and at Snežnica (Mg: 3400 ppm in matrix and 3220 ppm in infills). In spite of vertical variability and small-scale patchiness in preservation, microtexture of mudstones and wackestones at Strapková is more affected by silicification than at Brodno and Snežnica (Fig. 3).

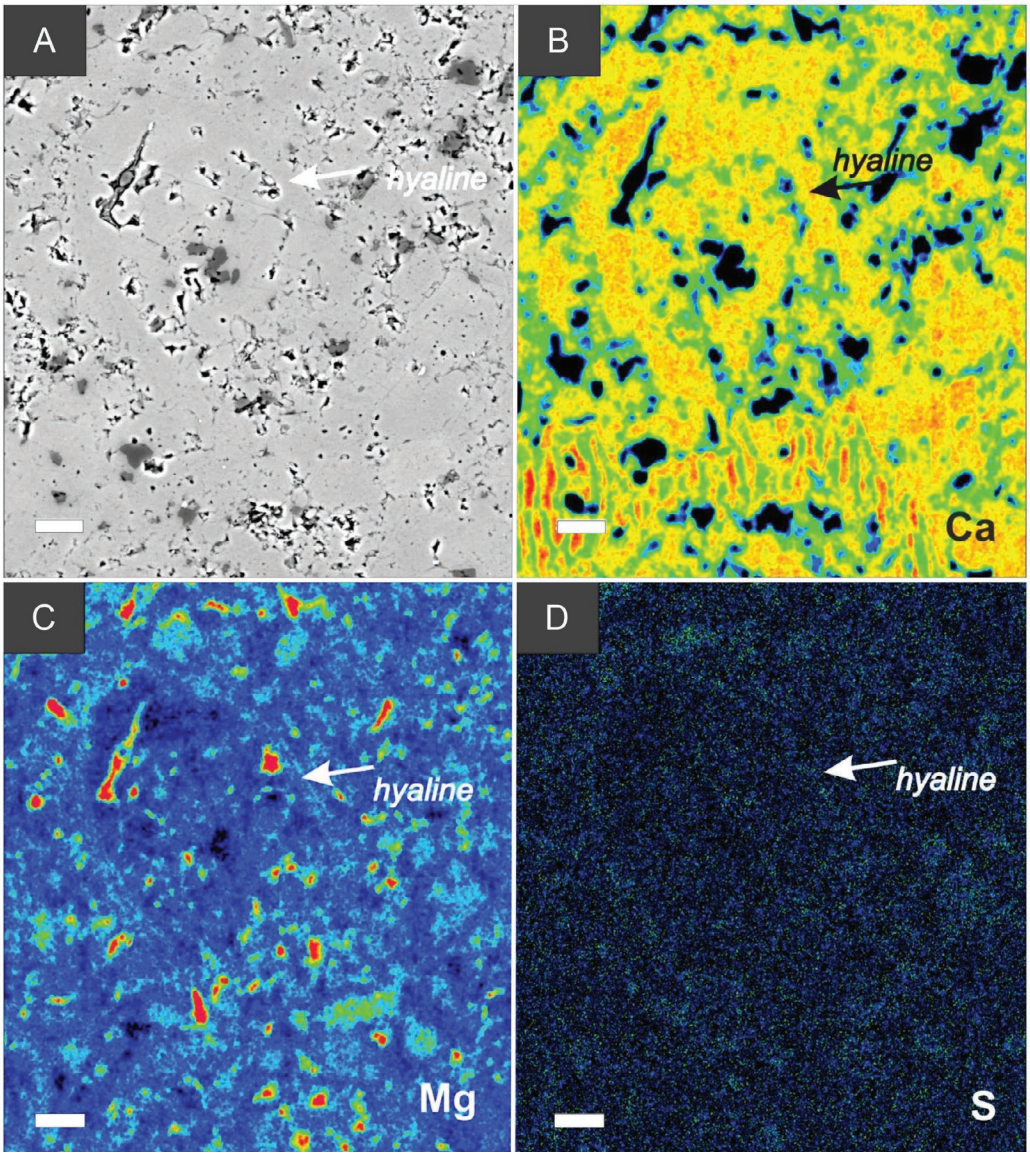

Fig. 9. BSE and the corresponding electron microprobe maps showing that the hyaline layer of *Crassicollaria* is magnesium-rich (Mg) and the adjacent matrix has slightly impoverished in Mg concentration. **(A–D)** Lorica of *Crassicollaria* with a hyaline layer. Snežnica (bed 19.25 middle). The change from blue to red colours corresponds to an increase in the concentration of each element (Ca, Mg and S). Scale=10 µm.

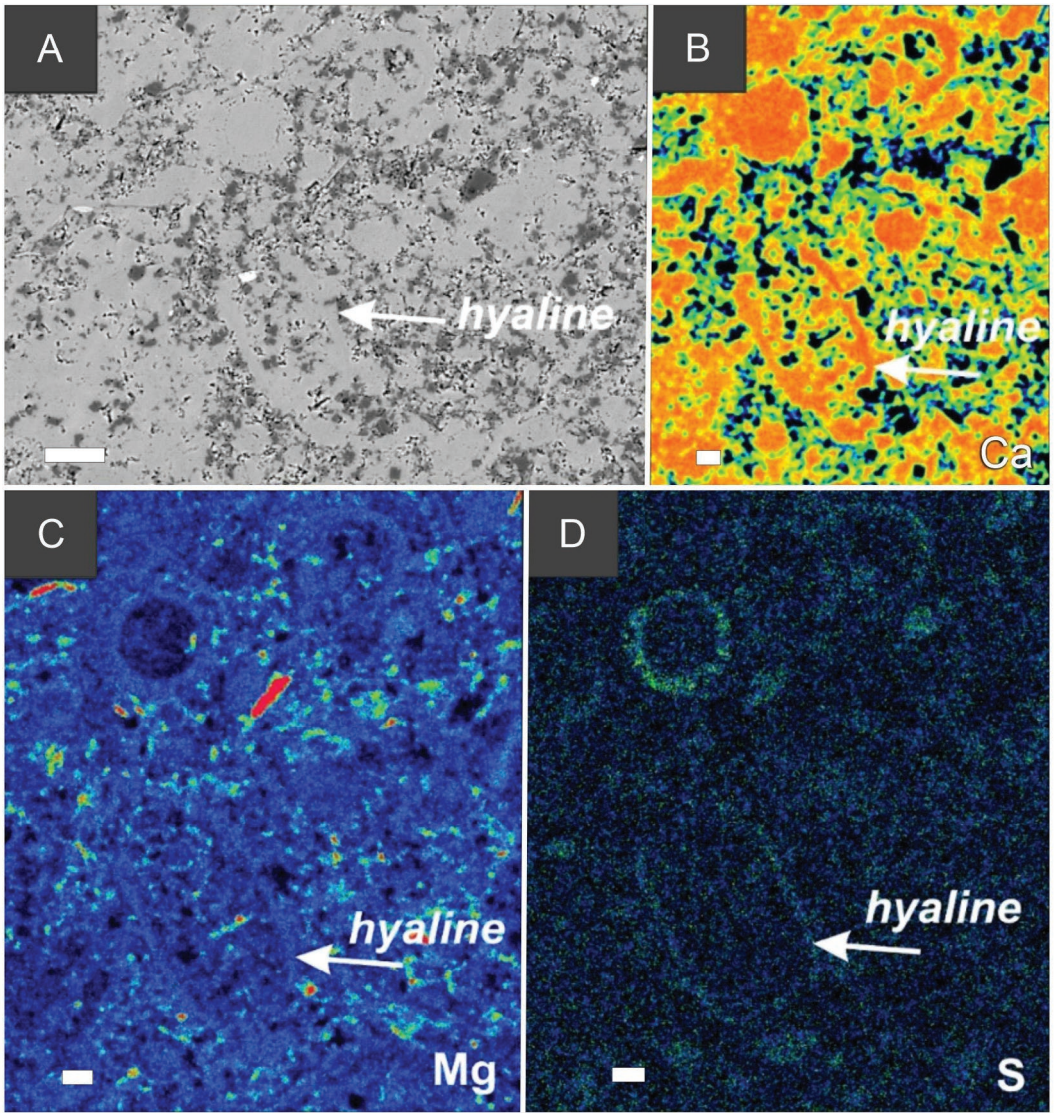

Fig. 10. BSE and electron microprobe maps showing that the hyaline layer of *Crassicollaria* and adjacent dinocyst is sulphur-poor (S) and magnesium-rich (Mg), the adjacent matrix affected by extensive silicification has the smaller content of Mg concentration than the hyaline layer. **(A–D)** Lorica of *Crassicollaria* with a hyaline layer. The sample is from Strapková (bed 291.32). The change from blue to red colours corresponds to an increase in the concentration of each element (Ca, Mg and S). Scale=10 μm.

Discussion

Diagenetic modification of pelagic oozes

The microtexture and the preservation of sedimentary particles and cements show that pelagic mudstones and wackestones of the Czorszstyn and Pieniny Limestone formations generally consist of loosely- to densely-packed pelagic skeletal remains that are predominantly composed of nannofossils (as also observed by Busson & Noël 1991) and microplankton (dinocysts and calpionellids, Fig. 3C, D). With the exception of well-sorted calciturbiditic beds at Snežnica, identifiable skeletal remains from shelf environments are rare or absent in these facies. The main pelagic components include tests of microplankton (calpionellids and dinocysts, and other groups as globochaetes, *Saccocoma,* and calcitized radiolarians) and nannofossils (coccoliths and nannoliths), which are represented relatively complete specimens, identifiable fragments (e.g., Fig. 3A, B), or by aggregates of very small 2–3 μm-long particles that probably represent non-identifiable nannofossil remains. Importantly, the interspaces among well-visible nannoplankton remains, calpionellids or dinocysts are filled by 2–10 μm-long micritic or microsparitic crystals with straight surfaces (Fig. 3C, D), probably representing an early-diagenetic cement, similar to that observed in the Tithonian–Berriasian deposits of the Magellan Rise (Schlanger et al. 1973). The cementation that occluded pore spaces within tests of pelagic remains likely occurred relatively early during shallow burial, as tests of calpionellids or radiolarians are mostly uncompacted.

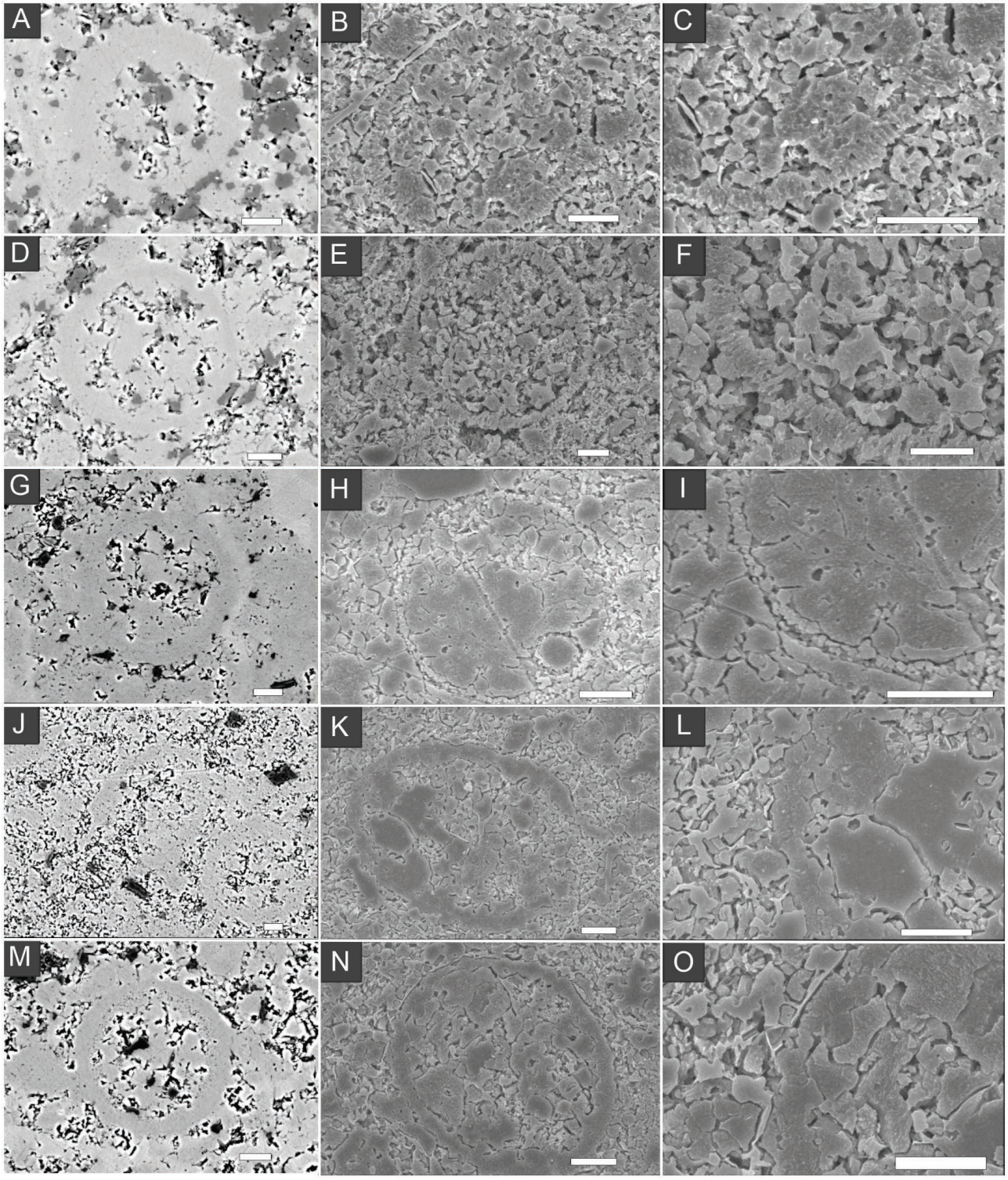

Fig. 11. Ultrastructure of *Calpionella* with the hyaline layer in specimens photographed with BSE (left column) and SEM (middle and right column). **(A)** Bed ST 290 (Strapková, *Remanei* Subzone). **(B, C)** Bed BR 8A (Brodno, *Remanei* Subzone). **(D)** Bed ST 290,32 (Strapková, *Remanei* Subzone). **(E, F)** Bed BR 27E (Brodno, *Alpina* Subzone). **(G)** Bed Sn 19.25 middle part (Snežnica, *Remanei* Subzone). **(H, I)** Bed Sn 19.24 (Snežnica, *Remanei* Subzone). **(J)** Bed BR 10 up (Brodno, *Intermedia* Subzone). **(K, L)** Bed ST 291,32 (Strapková, *Remanei* Subzone). **(M)** Bed Sn 19.25 base (Snežnica, *Remanei* Subzone). **(N, O)** Bed ST 291,32 (Strapková, *Remanei* Subzone). Scale=10 μm.

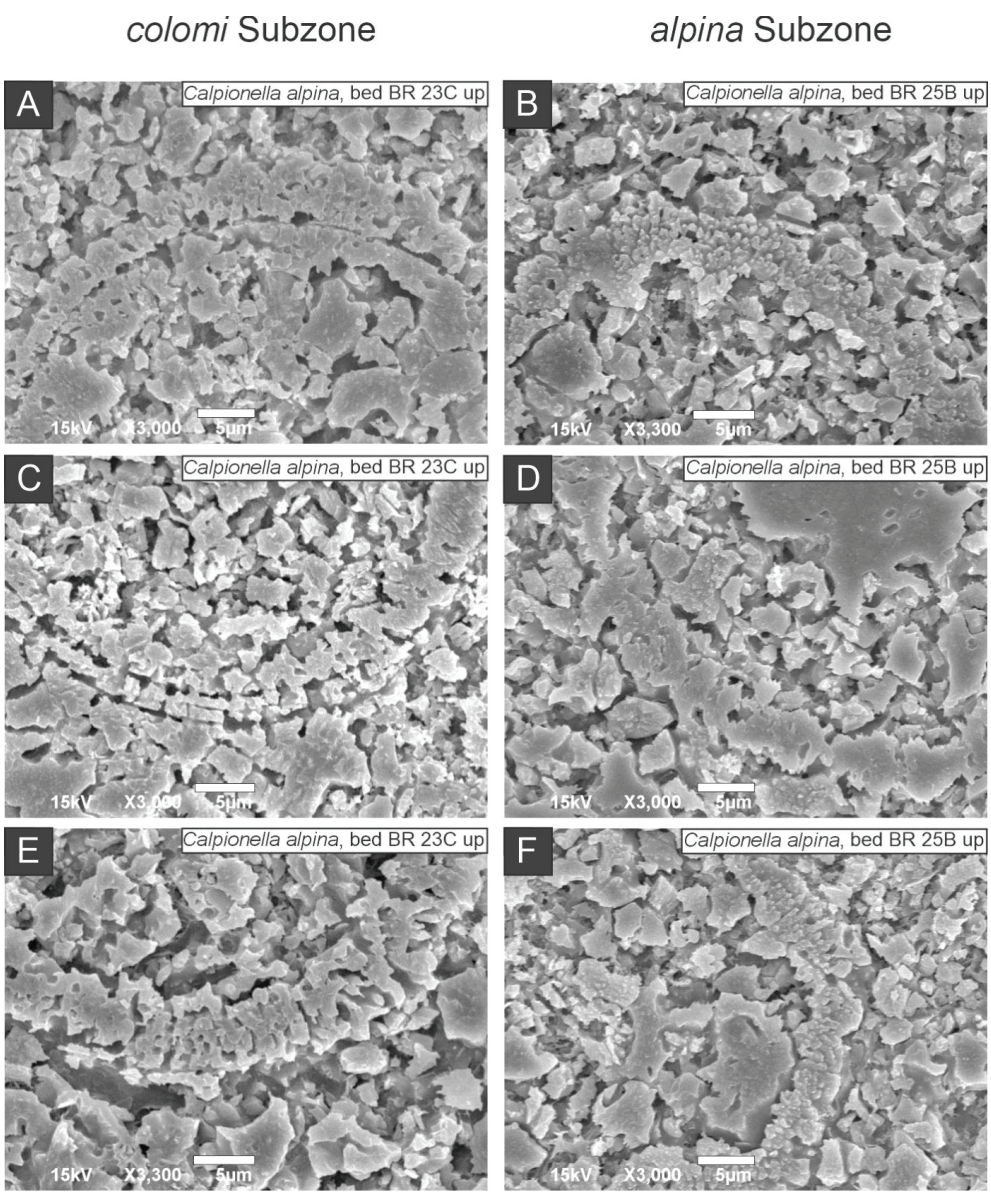

Fig. 12. Preservation of *Calpionella alpina,* with a signature of multiple sheets within the hyaline layer. **(A, C, E)** Two or even three sheets or layers of crystals in the hyaline layer of *Calpionella alpina* in the *Colomi* Subzone at Brodno (upper part of bed 23C). **(B, D, F)** Sections of the hyaline layer of *Calpionella alpina* in the *Alpina* Subzone at Brodno where crystals are sectioned transversally relative to their longer direction (upper part of bed 25B). The irregular thickness of the lorica walls indicate the effects of dissolution. Scale=5 µm.

The contribution of aragonite dissolution to cement precipitation in near-surface diagenetic zone during this initial early-diagenetic phase was probably limited because the initial abundance of originally-aragonitic bioclasts was probably rather low. This inference is based on the very rare or absent moldic preservation, which is restricted to occasional fragments of ammonites or other molluscs in the Czorsztyn Formation. The concentrations of Sr in lorica infills and in the external micritic sediment are very low (less than 300 ppm), with Sr/Ca is consistently below 0.45 at all sections, as is typical of pelagic carbonates formed by calcitic nannofossils and foraminifers (Ando et al. 2006). Nevertheless, remains of low-Mg calcitic microplankton and nannoplankton were also affected by dissolution. First, calpionellid loricae in particular, exhibit markedly irregular and locally very thin wall thicknesses, partial dissolution, even though the overall proportion of dissolved test walls is rather minor. Second, nannofossils are frequently preserved as incomplete or corroded fragments and the total nannofossil assemblages at Brodno and Strapková are dominated by dissolution-resistant genera such as *Watznaueria*, *Conusphaera*, *Polycostella* and *Nannoconus* (Michalík et al. 2009, 2016), indicating a bias against fragile and small nannoplankton species. Therefore, the dissolution of nano- and micrometric calcitic crystals constituting tests of these planktonic taxa could have contributed to cement precipitation (e.g., via Ostwald ripening where the smallest crystals

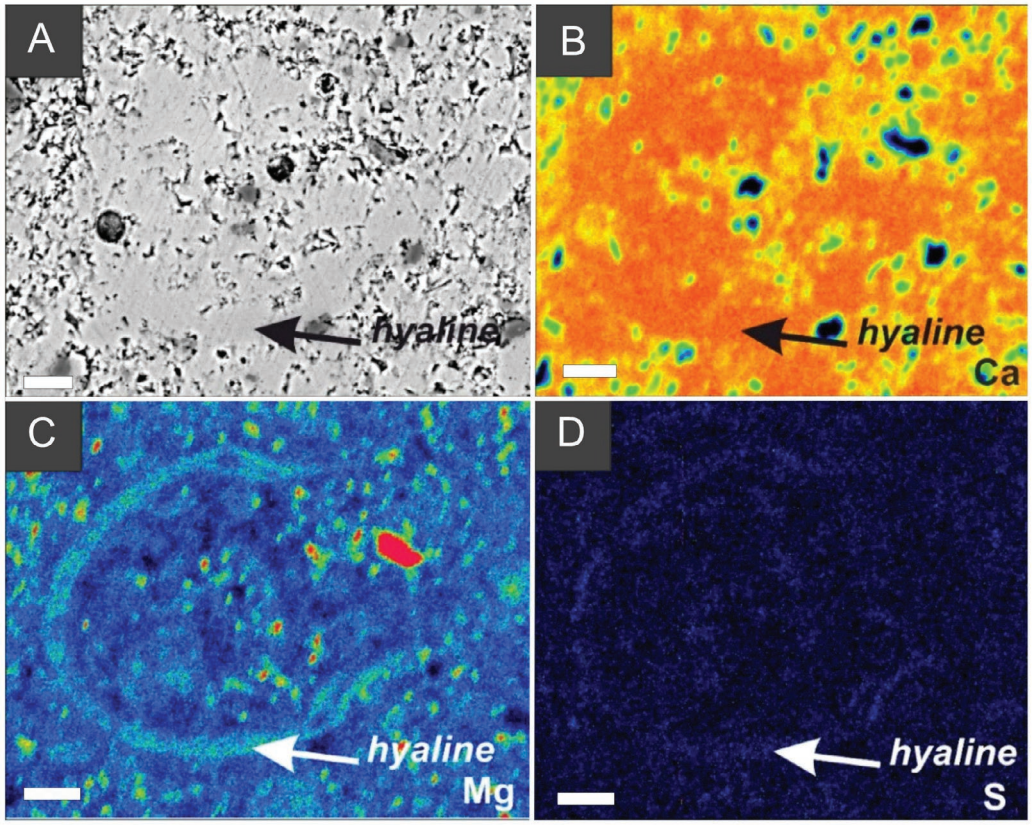

Fig. 13. BSE and electron microprobe maps showing that the hyaline layer of *Calpionella* is enriched in sulphur (S) and magnesium (Mg), and the adjacent matrix and the test infill have lower Mg concentrations. **(A–D)** Lorica of *Calpionella* with a hyaline layer. Brodno (bed 24C upper part, *Alpina* Subzone). The change from blue to red colours corresponds to an increase in the concentration of each element (Ca, Mg and S). Scale=10 μm.

are preferentially dissolved, Morse & Casey 1988; Volery et al. 2010; although Lucia 2017 did not find any evidence for size selectivity of dissolution). A similar process has been postulated for the diagenesis of hemi- or eupelagic oozes that are transformed to chalks and ultimately to limestones (Mattioli 1997; Frank et al. 1999). This early-diagenetic (shallow-burial) phase, represented by calcite dissolution and the precipitation of micritic and microsparitic calcitic cements in pore spaces, was associated with the release of Mg from high-Mg calcitic echinoderm. This process led to the precipitation of microdolomitic grains within echinoderm ossicles and along their syntaxial rims (Fig. 2D), indicating that this phase occurred in a closed diagenetic system. The enrichment of Mn in micritic and microsparitic cements further indicates that the initial cementation phase took place under reducing conditions.

Low-Mg calcitic calpionellid loricae and adjacent micritic or microsparitic cements are in some cases affected by aggrading neomorphism, leading to coarser crystals and loss of inter-crystalline boundaries within tests and on the interface of tests with adjacent cements, with crystals cutting across pelagic tests and cement crystals. This neomorphic phase probably postdates the early cementation phase. In some cases, individual coccoliths and nannoliths also tend to gradually pass into microsparitic crystals without any distinct inter-crystalline boundaries, indicating that small-scale aggrading neomorphism followed the initial cementation and dissolution phase (Fig. 2D). The neomorphic phase was ultimately followed by the precipitation of authigenic, euhedral to subhedral quartz and albite that locally replace calpionellid tests but typically filled residual pores or replaced micritic crystals (during deeper-burial chemical compaction and pressure dissolution). Diagenetic pathways leading to the formation of biancone and maiolica deposits are thus similar to other pelagic deposits predominantly formed by low-Mg calcitic remains that passed through the chalk-limestone transition, leading to a decrease in porosity and an increase in the proportion of cements and neomorphosed remains. These processes in turn reduced the abundance of the finest micrite (e.g., Westphal et al. 2004; Beltran et al. 2009; Lucia 2017; Munnecke et al. 2023), the overall abundance of identifiable nannofossils, and the percentage of dissolution-sensitive nannofossils (e.g., Saïag et al. 2019).

Preservation of hyaline layer

Several lines of evidence indicate that the loricae were partly or locally affected by small-scale dissolution, cement overgrowth, and aggrading neomorphism. The variability in

wall thickness within individual loricae result of localized dissolution (reducing the thickness), overgrowth at other places (increasing the thickness), and crystal coarsening and amalgamation (associated with the loss of inter-crystalline boundaries). The size and shape of crystals in the hyaline layer are probably biased up as the consequence of neomorphism that can increase crystal size. Aubry et al. (1975) reported that crystal sizes in calpionellids (including *Calpionella alpina*) reached 0.3–0.4 µm in the Tithonian of Tunisia whereas crystal sizes documented here usually exceed 0.5 µm and on average around 1 µm. This difference probably reflects a higher degree of neomorphism of loricae in the Tithonian and Berriasian mudstones and wackestones in the Western Carpathians. Nevertheless, despite these neomorphic effects and local replacement by authigenic microquartz, calpionellids tests generally retain the original chemical composition, characterized by higher concentrations of Mg and S than in micrite and microsparite (with nannofossil remains).

Differences in ultrastructure between genera and evolutionary transitions

Despite diagenetic modification, the ultrastructure of the hyaline layer differs among genera. When comparing the size and shape of the lorica-forming in *Praetintinnopsella*, *Crassicollaria*, and *Calpionella*, crystals in *Praetintinnopsella* and *Crassicollaria* are equidimensional and tightly clustered around 1 µm in length and width (Fig. 5), whereas crystals in *Calpionella* are more elongated and broader (Fig. 5). Therefore, the processes such as cementation, small-scale dissolution or neomorphism did not significantly homogenize the ultrastructure of tests of *Praetintinnopsella*, *Crassicollaria* and *Calpionella* (Fig. 14) preserved in pelagic ooze deposits with a similar diagenetic history. As observed by Ölveczká et al. (2024), *Praetintinnopsella* does not possess the microgranular layer that is typical of *Chitinoidella*, although further investigation of semichitinoidellid loricae is required to clarify the evolutionary and structural transition between the microgranular and hyaline layers. However, the hyaline layer in *Praetintinnopsella* closely resembles that of *Crassicollaria* (Fig. 5A). The similarity in crystal size of *Praetintinnopsella* and *Crassicollaria* supports the hypothesized evolutionary relationship between these genera (e.g., Houša 1990). Some specimens of the genus *Crassicollaria*, a very thin, dark rim (ca. 0.8 µm-thick) occurs on the outer surface of the hyaline layer (Fig. 3G, H; Fig. 8E, F). It is possible that this rim represents a postmortem microbial coating. In contrast to *Crassicollaria*, the hyaline layer of *Calpionella* is characterized by larger crystals and thus by smaller surface area-to-volume crystal ratio. As abundance of *Calpionella* species increased and that of *Crassicollaria* declined during the late Tithonian, the evolution of the hyaline layer appears to record

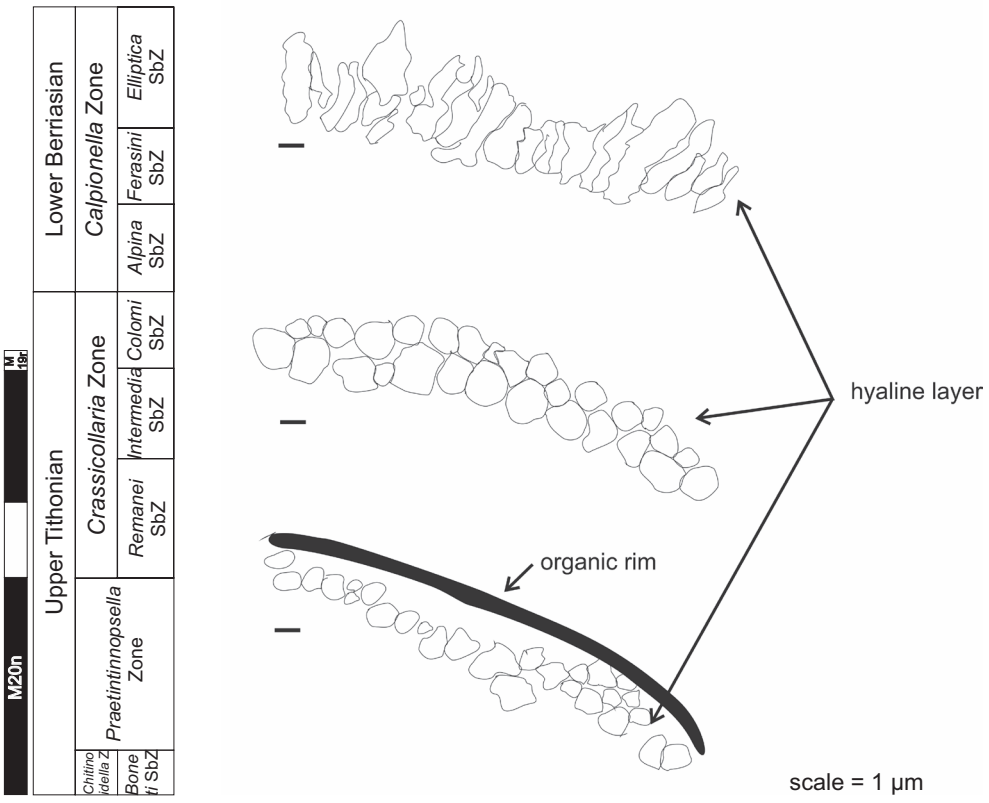

Fig. 14. Temporal changes in the lorica ultrastructure of *Praetintinnopsella*, *Crassicollaria*, and *Calpionella* during the Late Tithonian and Early Berriasian (as observed in their longitudinal lorica sections), with the stratigraphic distribution as observed at the Brodno section. The shape of crystals is partly affected by small-scale dissolution and aggrading neomorphism.

a trend towards stronger calcification, reflecting a shift from organic-poor to more carbonate-rich tests (Fig. 14). Whether this evolutionary shift toward organic-poor and carbonate-rich tests is related to changes in temperature, seawater carbonate saturation state, Ca concentration, or other environmental factors remains to be investigated.

Differences in preservation among three successions

Ölveczká et al. (2024) observed that microgranular layer of *Chitinoidella* is more altered at Strapková (Orava Succession, possibly originally located in the Fatric Unit) than at Brodno or Snežnica (Pieniny–Kysuca Succession), showing stronger packing and larger crystal size at Strapková. SEM observations further indicate that the hyaline layer of *Crassicollaria* and *Calpionella* are also less well-preserved at Strapková. Our BSE and SEM observations further show that Mn concentrations are higher, and authigenic (euhedral to subhedral) microquartz (locally also replacing calcitic tests of calpionellids) is more frequent at Strapková than at Brodno and Snežnica. The bulk-rock isotopic composition investigated by Michalík et al. (2009) at Brodno and by Michalík et al. (2016) at Strapková show a positive correlation between $\delta^{13}C$ and $\delta^{18}O$ at Strapková ($r=0.36$, $p=0.005$) and the lack of correlation at Brodno ($r=-0.004$, $p=0.97$). The $\delta^{18}O$ values are slightly more negative at Strapková (mean=−1.8 ‰ in the Czorsztyn Formation and −1.96 ‰ in the Pieniny Formation) than at Brodno (mean=−1.65 ‰ in the Czorsztyn Formation and −1.84 ‰ in the Pieniny Formation). These patterns indicate higher burial temperature at Strapková, and are consistent with inferences that place its origin in the Fatric Unit that is uniformly affected by higher degree of diagenetic modifications than the successions of the Pieniny Klippen Belt (such as the Czorsztyn or Pieniny–Kysuca successions). For example, Mišík (1995) observed higher frequency of authigenic quartz in Jurassic limestones in the Fatric Unit than in the Pieniny Klippen Belt.

Conclusion

Pelagic mudstones and wackestones of the Czorsztyn and Pieniny Limestone formations are formed by a mixture of microplankton tests, complete and fragmented (mainly dissolution-resistant) nannoplankton tests, and primarily cement-forming micritic and microsparitic crystals. Morphological differences among *Praetintinnopsella*, *Crassicollaria*, and *Calpionella* are associated with ultrastructural differences in the development of their hyaline layers. The ultrastructure of the hyaline layer in *Praetintinnopsella* is more similar to that of *Crassicollaria* than to *Calpionella*. Crystals in *Praetintinnopsella* and *Crassicollaria* are relatively equidimensional and approximately 1 μm in length (resulting in a higher surface area-to-volume ratio), whereas those in *Calpionella* are more elongated, about 2.2 μm long (with smaller surface area-to-volume ratio). The similarity in the microstructure of the hyaline layer supports a close phylogenetic relation between *Praetintinnopsella* and *Crassicollaria,* and changes in the size and shape of crystals document a trend towards stronger calcification during the late Tithonian.

Although the calpionellid loricae are affected by small-scale dissolution and overgrowth and by minor aggrading neomorphism, these processes did not markedly alter their chemical composition. The loricae remain enriched in magnesium and sulphur and depleted in manganese relative to the pore- and void-filling micritic or microsparitic cement as well as to non-identifiable micritic grains in the sediment matrix. We infer that the initial diagenetic phase involved the dissolution of low-Mg calcitic (micro- and nannoplankton) remains, precipitation of micritic and microsparitic cements in pore spaces and in lorica interiors, and the release of Mg from rare echinoderm ossicles followed by precipitation of microdolomite. This phase was followed by a phase with aggrading neomorphism and ultimately by a phase with the precipitation of authigenic quartz and albite. Although the Tithonian and Berriasian pelagic deposits of the Czorsztyn and Pieniny Limestone formations were affected by early-diagenetic transformations and by silicification, these processes were localized and did not obliterate between-genus difference in the test ultrastructure and the differences in the chemical composition between loricae and adjacent micritic grains and/or crystals.

Acknowledgements: We thank to editor and all reviewers for the advice and guidance that led to the improvement of the article. We thank Dr. Sergyi Kurylo for his assistance with the microprobe measurements. This study was supported by the Slovak Scientific Grant Agency (VEGA 2/0106/23 and VEGA 2/0012/24), Slovak Research and Development Agency (APVV 22/0523) and by the DoktoGrant of the Slovak Academy of Sciences (APP0526).

References

Ando A., Kawahata H. & Kakegawa T. 2006: Sr/Ca ratios as indicators of varying modes of pelagic carbonate diagenesis in the ooze, chalk and limestone realms. *Sedimentary Geology* 191, 37–53. https://doi.org/10.1016/j.sedgeo.2006.01.003

Aubry M.P., Bignot G., Bismuth H. & Remane J. 1975: Premiers résultats de l´observation au M.E.B. de la lorica des calpionelles et de quelques microfossiles qui leur sont associés. *Revue Micropaleontologie* (Paris) 18, 127–133.

Aubry M.P., Bord D., Beaufort L., Kahn A. & Boyd S. 2005: Trends in size changes in the coccolithophorids, calcareous nannoplankton, during the Mesozoic: A pilot study. *Micropaleontology* 51, 309–318. https://doi.org/10.2113/gsmicropal.51.4.309

Beltran C., de Rafélis M., Person A., Stalport F. & Renard M. 2009: Multiproxy approach for determination of nature and origin of carbonate micro-particles so-called “micarb” in pelagic sediments. *Sedimentary Geology* 213, 64–76. https://doi.org/10.1016/j.sedgeo.2008.11.004

Benzaggagh M. 2020: Discussion on the calpionellid biozones and proposal of a homogeneous calpionellid zonation for the Tethyan Realm. *Cretaceous Research* 114, 104184. https://doi.org/10.1016/j.cretres.2019.07.014

Benzaggagh M. 2021: Systematic revision and evolution of the Tithonian family Chitinoidellidae Trejo, 1975. *Carnets de géologie* 21, 27–53. https://doi.org/10.2110/carnets.2021.2102

Bernoulli D. & Jenkyns H.C. 2009: Ancient oceans and continental margins of the Alpine-Mediterranean Tethys: Deciphering clues from Mesozoic pelagic sediments and ophiolites. *Sedimentology* 56, 149–190. https://doi.org/10.1111/j.1365-3091.2008.01017.x

Bolli H.M. 1980: Calcisphaerulidae and Calpionellidae from the Upper Jurassic and Lower Cretaceous of D.S.D.P. Hole 416A, Moroccan Basin. In: Lancelot Y. et al.: *Deep Sea Drilling Project, Washington, Initial Reports* 50, 1–7, 525–543. https://doi.org/10.2973/dsdp.proc.50.115.1980

Bornemann A., Aschwer U. & Mutterlose J. 2003: The impact of calcareous nannofossils on the pelagic carbonate accumulation across the Jurassic–Cretaceous boundary. *Palaeogeography, Palaeoclimatology, Palaeoecology* 199, 187–228. https://doi.org/10.1016/S0031-0182(03)00507-8

Boughdiri M., Sallouhi H., Maalaoui K., Soussi M. & Cordey F. 2006: Calpionellid zonation of the Jurassic–Cretaceous transition in North-Atlasic Tunisia. Updated stratigraphy of the "Tunisian trough" and Upper Jurassic regional correlations. *Comptes Rendus Geoscience* 338, 1250–1259. https://doi.org/10.1016/j.crte.2006.09.015

Bralower T.J., Monechi S. & Thierstein H.R. 1989: Calcareous nannofossils zonation of the Jurassic–Cretaceous boundary interval and correlations with the Geomagnetic Polarity Timescale. *Marine Micropaleontology* 14, 153–235. https://doi.org/10.1016/0377-8398(89)90035-2

Busson G. & Noël D. 1991: Les nannoconidés, indicateurs environnementaux des océans et mers épicontinentales du Jurassique terminal et du Crétacé inférieur. *Oceanologica Acta* 14, 333–356.

Casellato C.E. 2010: Calcareous nannofossil biostratigraphy of upper Callovian–lower Berriasian successions from the southern Alps, north Italy. *Rivista Italiana di Paleontologia e Stratigrafia* 116, 3. https://doi.org/10.13130/2039-4942/6394

Casellato C.E. & Erba E. 2021: Reliability of calcareous nannofossil events in the Tithonian-early Berriasian time interval: Implications for a revised high resolution zonation. *Cretaceous Research* 117, 104611. https://doi.org/10.1016/j.cretres.2020.104611

Duchamp-Alphonse S., Fiet N., Pagel M. & Jürgen R. 2009: A chemical method for extracting calpionellids from indurated calcareous rocks. *Micropaleontology* 55, 87–93. https://doi.org/10.47894/mpal.55.1.07

Erba E., Bottini C., Faucher G., Gambacorta G. & Visentin S. 2019: The response of calcareous nannoplankton to Oceanic Anoxic Events: The Italian pelagic record. *Bollettino della Società Paleontologica Italiana* 58, 51–71. https://doi.org/10.4435/BSPI.2019.08

Főzy I., Janssen N.M. & Price G.D. 2011: High-resolution ammonite, belemnite and stable isotope record from the most complete Upper Jurassic section of the Bakony Mts (Transdanubian Range, Hungary). *Geologica Carpathica* 62, 413–433. https://doi.org/10.2478/v10096-011-0030-y

Frank T.D., Arthur M.A. & Dean W.E. 1999: Diagenesis of Lower Cretaceous pelagic carbonates, North Atlantic; paleoceanographic signals obscured. *The Journal of Foraminiferal Research* 29, 340–351.

Grabowski J., Haas J., Stoykova K., Wierzbowski H. & Branski P. 2017: Environmental changes around the Jurassic/Cretaceous transition: New nannofossil, chemostratigraphic and stable isotope data from the Lokút section (Transdanubian Range, Hungary). *Sedimentary Geology* 360, 54–72. https://doi.org/10.1016/j.sedgeo.2017.08.004

Grabowski J., Bakhmutov V., Kdýr S., Krobicki M., Pruner P., Reháková D., Schnabl P., Stoykova K. & Wierzbowski H. 2019: Integrated stratigraphy and palaeoenvironmental interpretation of the Upper Kimmeridgian to Lower Berriasian pelagic sequences of the Velykyi Kamianets section (Pieniny Klippen Belt, Ukraine). *Palaeogeography, Palaeoclimatology, Palaeoecology* 532, 109–216. https://doi.org/10.1016/j.palaeo.2019.05.038

Grandesso P. 1977: Gli strati a precalpionellidi del Titoniano ei loro rapporti con il Rosso Ammonitico Veneto. *Memoire di Scienze Geologiche* 32, 1–14.

Granier B.R., Ferry S. & Benzaggagh M. 2023: Hiatuses and redeposits in the Tithonian–Berriasian transition at Le Chouet (Les Près, La Drôme, SE France): Sedimentological and biostratigraphical implications. *Carnets Geol.* 23, 123–147.

Houša V. 1990: Stratigraphy and calpionellid zonation of Stramberg Limestone and associated Lower Cretaceous beds. In: Pallini G., Cecca F., Cresta S. & Santantonio M. (Eds.): Atti del secondo convegno internazionale: Fossili, Evoluzione, Ambiente, Pergola 1987. *Comitato Centenario Raffaele Piccinini, Pergola*, 365–370.

Houša V., Krs M., Krsová M. & Pruner P. 1996: Magnetostratigraphic and micropaleontological investigations along the Jurassic/Cretaceous boundary strata, Brodno near Žilina (Western Slovakia). *Geologica Carpathica* 47, 135–151.

Houša V., Krs M., Krsová M., Man O., Pruner P. & Venhodová D. 1999: High-resolution magnetostratigraphy and micropalaeontology across the J/K boundary strata at Brodno near Žilina, western Slovakia: summary of results. *Cretaceous Research* 20, 699–717. https://doi.org/10.1006/cres.1999.0177

Kaczmarek S.E., Fullmer S.M. & Hasiuk F.J. 2015: A universal classification scheme for the microcrystals that host limestone microporosity. *Journal of Sedimentary Research* 85, 1197–1212. https://doi.org/10.2110/jsr.2015.79

Kälin O. & Bernoulli D. 1984: *Schizosphaerella* Deflandre and Dangeard in Jurassic deeper-water carbonate sediments, Mazagan continental-margin (Hole-547B) and Mesozoic Tethys. *Initial Reports of the Deep Sea Drilling Project* 79, 411–435. https://doi.org/10.2973/dsdp.proc.79.112.1984

Katz M.E., Finkel Z.V., Grzebyk D., Knoll A.H. & Falkowski P.G. 2004: Evolutionary trajectories and biogeochemical impacts of marine eukaryotic phytoplankton. *Annual Review of Ecology, Evolution, and Systematics* 35, 523–556. https://doi.org/10.1146/annurev.ecolsys.35.112202.130137

Kietzmann D.A. & Scasso R.A. 2020: Jurassic to Cretaceous (upper Kimmeridgian–? Lower Berriasian) calcispheres from high palaeolatitudes on the Antarctic Peninsula: local stratigraphic significance and correlations across Southern Gondwana margin and the Tethyan realm. *Palaeogeography, Palaeoclimatology, Palaeoecology* 537, 109419. https://doi.org/10.1016/j.palaeo.2019.109419

Kietzmann D.A., Iglesia Llanos M.P., Gonzalez-Tomassini F., Lanusse Noguera I., Vallejo D. & Reijenstein H. 2021: Upper Jurassic–Lower Cretaceous calpionellid zones in the Neuquén Basin (Southern Andes, Argentina): Correlation with ammonite zones and biostratigraphic synthesis. *Cretaceous Research* 127, 104950. https://doi.org/10.1016/j.cretres.2021.104950

Kietzmann D.A., Iglesia Llanos M.P. & Iovino F. 2023: Tithonian–Berriasian calcisphere (calcareous dinoflagellate cysts) zones in the Neuquén Basin, Argentina: correlation between Southern Andes and Tethyan regions. *Newsletters on Stratigraphy* 56, 157–185. https://doi.org/10.1127/nos/2022/0729

Knoll A.H. & Follows M.J. 2016: A bottom-up perspective on ecosystem change in Mesozoic oceans. *Proceedings of the Royal Society B: Biological Sciences* 283, 20161755. https://doi.org/10.1098/rspb.2016.1755

Kowal-Kasprzyk J. & Reháková D. 2019: A morphometric analysis of loricae of the genus Calpionella and its significance for the Jurassic/Cretaceous boundary interpretation. *Newsletter on Stratigraphy* 52, 33–54. https://doi.org/10.1127/nos/2018/0461

Lakova I. 1993: Middle Tithonian to Berriasian praecalpionellid and calpionellid zonation of the Western Balkanides, Bulgaria. *Geologica Balcanica* 23, 3–24. https://doi.org/10.52321/GeolBalc.23.6.3

Lakova I., Stoykova K. & Ivanova D. 1999: Calpionellid, nannofossil and calcareous dinocyst bioevents and integrated biochronology of the Tithonian to Valanginian in the Western Balkanides. Bulgaria. *Geologica Carpathica* 50, 151–168.

Lodowski D.G., Szives O., Virag A. & Grabowski J. 2024: The latest Jurassic–earliest Cretaceous climate and oceanographic changes in the Western Tethys: the Transdanubian Range (Hungary) perspective. *Sedimentology* 71, 1705–2065. https://doi.org/10.1111/sed.13194

López-Martínez R., Barragán R. & Reháková D. 2013: The Jurassic/Cretaceous boundary in the Apulco area by means of calpionellids and calcareous dinoflagellates: An alternative to the classical Mazatepec section in eastern Mexico. *Journal of South American Earth Sciences* 47, 142–151. https://doi.org/10.1016/j.jsames.2013.07.009

Lucia F.J. 2017: Observations on the origin of micrite crystals. *Marine and Petroleum Geology* 86, 823–833. https://doi.org/10.1016/j.marpetgeo.2017.06.039

Lukeneder A., Halasova E., Kroh A., Mayrhofer S., Pruner P., Rehakova D., Schnabl P., Sprovieri M. & Wagreich M. 2010: High resolution stratigraphy of the Jurassic–Cretaceous boundary interval in the Gresten Klippenbelt (Austria). *Geologica Carpathica* 61, 365–381. https://doi.org/10.2478/v10096-010-0022-3

Mattioli E. 1997: Nannoplankton productivity and diagenesis in the rhythmically bedded Toarcian–Aalenian Fiuminata section (Umbria-Marche Apennine, central Italy). *Palaeogeography, Palaeoclimatology, Palaeoecology* 130, 113–133. https://doi.org/10.1016/S0031-0182(96)00127-7

Michalík J. & Reháková D. 2011: Possible markers of the Jurassic/Cretaceous boundary in the Mediterranean Tethys: A review and state of art. *Geoscience Frontiers* 2, 475–490. https://doi.org/10.1016/j.gsf.2011.09.002

Michalík J., Reháková D. & Peterčáková M. 1990: Ku stratigrafii hraničných jursko-kriedových súvrství v kysuckej sekvencii bradlového pásma Západných Karpát, profil Brodno pri Žiline [To the stratigraphy of Jurassic–Cretaceous boundary beds in the Kysuca sequence of the West Carpathian Klippen Belt, Brodno section near Žilina]. In: Biostratigrafické a sedimentologické studie v mezozoiku Českého masívu a Západních Karpat, 2. diel. *Knihovnička Zemního plynu a nafty* 9b, Moravské naftové doly, Hodonín, 57–71.

Michalík J., Reháková D., Halásová E. & Lintnerová O. 2009: The Brodno section – a potential regional stratotype of the Jurassic/Cretaceous boundary (Western Carpathians). *Geologica Carpathica* 60, 213–232. https://doi.org/10.2478/v10096-009-0015-2

Michalík J., Reháková D., Grabowski J., Lintnerová O., Svobodová A., Schlögl J., Sobień K. & Schnabl P. 2016: Stratigraphy, plankton communities, and magnetic proxies at the Jurassic/Cretaceous boundary in the Pieniny Klippen Belt (Western Carpathians, Slovakia). *Geologica Carpathica* 67, 303–328. https://doi.org/10.1515/geoca-2016-0020

Michalík J., Reháková D., Lintnerová O., Halásová E. & Grabowski J. 2019: 1st Stop – Brodno section. In: XIVth Jurassica Conference & Workshop of the ICS Berriasian Group. *Field Trip Guide and Abstract Book*, 33–41.

Michalík J., Grabowski J., Lintnerová O., Reháková D., Kdýr Š. & Schnabl P. 2021: Jurassic–Cretaceous boundary record in Carpathian sedimentary sequences. *Cretaceous Research* 118, 104659. https://doi.org/10.1016/j.cretres.2020.104659

Mišík M. 1995: Authigenic quartz crystals in the Mesozoic and Paleogene carbonate rocks of the Western Carpathians. *Geologica Carpathica* 46, 227–239.

Morse J.W. & Casey W.H., 1988: Ostwald processes and mineral paragenesis in sediments. *American Journal of Science* 288, 537–560. https://doi.org/10.2475/ajs.288.6.537

Munnecke A., Wright V.P. & Nohl T. 2023: The origins and transformation of carbonate mud during early marine burial diagenesis and the fate of aragonite: a stratigraphic sedimentological perspective. *Earth-Science Reviews* 239, 104366. https://doi.org/10.1016/j.earscirev.2023.104366

Noël D. & Busson G. 1990: L'importance des schizosphères, stomiosphères, Conusphaera et Nannoconus dans la genèse des calcaires fins pélagiques du Jurassique et du Crétacé inférieur/Importance of schizospheres, stomiospheres, *Conusphaera* and *Nannoconus* in the genesis of Jurassic and Early Cretaceous fine-grained pelagic limestones. *Sciences Géologiques, Bulletins et mémoires* 43, 63–93.

Nowak W.A. 1978: *Semichitinoidella* n. gen.(Tintinnina) of the Upper Jurassic of the Czorsztyn Succession, Pieniny Klippen Belt (Carpathians, Poland). *Annales Societatis Geologorum Poloniae* 48, 3–25.

Ölveczká D., Tomašových A., Reháková D., Schlögl J. & Michalík J. 2024: Assessing temporal transition between microgranular and hyaline tests of calcareous microplankton during the Late Jurassic. *Marine Micropaleontology* 190, 102379. https://doi.org/10.1016/j.marmicro.2024.102379

Petrova S., Rabrenović D., Lakova I., Koleva-Rekalova E., Ivanova D., Metodiev L. & Malešević N. 2012: Biostratigraphy and microfacies of the pelagic carbonates across the Jurassic/Cretaceous boundary in eastern Serbia (Stara Planina–Poreč Zone). *Geologica Balcanica* 41, 53–76. https://doi.org/10.52321/GeolBalc.41.1-3.53

Petrova S., Andreeva P., Metodiev L., Reháková D., Michalík J. & Lakova I. 2017: Calpionellid biostratigraphy and microfacies analysis of a Tithonian–Berriasian carbonate succession in the Western Srednogorie (Bulgaria). *Geologica Balcanica* 46, 65–92. https://doi.org/10.52321/GeolBalc.46.1.65

Petrova S., Reháková D., Erba E. & Grabowski J. 2025: Tithonian–Berriasian calpionellid and calcareous dinocyst biostratigraphy, and microfacies in the Torre de' Busi section (Lombardian Basin, northern Italy). *Cretaceous Research* 176, 106180. https://doi.org/10.1016/j.cretres.2025.106180

Plašienka D. 2019: Linkage of the Manín and Klape units with the Pieniny Klippen Belt and Central Western Carpathians: balancing the ambiguity. *Geologica Carpathica* 70, 35–61. https://doi.org/10.2478/geoca-2019-0003

R Core Team 2024: R: A language and environment for statistical computing. R Foundation for Statistical Computing, Vienna, Austria. https://www.R-project.org/

Reháková D. 2002: *Chitinoidella* Trejo, 1975 in Middle Tithonian carbonate pelagic sequences of the West Carpathian Tethyan area. *Geologica Carpathica* 53, 369–379.

Reháková D. & Michalík J. 1992: Correlation of Jurassic–Cretaceous boundary beds in West Carpathian profiles. *Földtani Közlöny* 122, 51–66.

Reháková D. & Michalík J. 1993: Observations of ultrastructure of the Upper Jurassic and Lower Cretaceous calpionellid tests. *Geologica Carpathica* 44, 75–79.

Reháková D. & Michalík J. 1996: *Stomiosphaera* or *Orthopithonella*? *Cadosina* or *Obliquipithonella*? notes to ultrastructure and systematic position of some Jurassic–Cretaceous calcareous dinoflagellates from Western Carpathians. *Mineralia Slovaca* 28, 92–98.

Remane J. 1963: Les Calpionelles dans les couches de passage Jurassique–Crétacé de la fosse vocontienne. *Travaux de Laboratoire de Géologie, Grenoble* 39, 25–82.

Remane J. 1964: Untersuchungen zur Systematik und Stratigraphie der Calpionellen in den Jura-Kreide-Grenzschichten des Vocontischen Troges. *Palaeontographica Abteilung* 123, 1–57.

Remane J. 1985: Calpionellids. In: Bolli H.M., Saunders J.B. & Perch-Nielsen K. (Eds.): Plankton Stratigraphy. *Cambridge University Press*, London, 55–572.

Remane J. 1998: Calpionellids. In: Introduction to Marine Micropaleontology. *Elsevier*, 161–170. https://doi.org/10.1016/B978-044482672-5/50006-4

Saïag J., Collin P.Y., Sizun J.P., Herbst F., Faÿ-Gomord O., Chateau Smith C., Caline B. & Lasseur É. 2019: Classifying chalk microtextures: sedimentary versus diagenetic origin (Cenomanian–Santonian, Paris Basin, France). *Sedimentology* 66, 2976–3007. https://doi.org/10.1111/sed.12618

Schlanger S.O., Douglas R.G., Lancelot Y. & Moore T.C., jr. 1973: Fossil preservation and diagenesis of pelagic carbonates from the Magellan Rise, Central North Pacific Ocean. In: Winterer E.L., Ewing J.L. et al.: *Initial Reports of the Deep Sea Drilling Project* 17, 407–427.

Schlögl J., Aubrecht R. & Tomašových A. 2000: The first find of the Orava Unit in the Púchov section of the Pieniny Klippen Belt (Western Slovakia). *Mineralia Slovaca* 32, 45–54.

Tremolada F., Bornemann A., Bralower T. J., Koeberl C. & van de Schootbrugge B. 2006: Paleoceanographic changes across the Jurassic/Cretaceous boundary: the calcareous phytoplankton response. *Earth and Planetary Science Letters* 241, 361–371. https://doi.org/10.1016/j.epsl.2005.11.047

Vincent E., Lehmann R., Sliter W.V. & Westberg M.J. 1980: Calpionellids from the Upper Jurassic and Neocomian of deep sea drilling project Site 416, Moroccan basin, Eastern North Atlantic. *Deep Sea Drilling Initial Reports* 79, 439–465.

Vishnevskaya V. 2017: The Jurassic–Cretaceous boundary in Boreal Russia: radiolarian and calcareous dinoflagellate potential biomarkers. *Geological Quarterly* 61, 641–654. https://doi.org/10.7306/gq.1370

Volery C., Davaud E., Durlet C., Clavel B., Charollais J. & Caline B. 2010: Microporous and tight limestones in the Urgonian Formation (late Hauterivian to early Aptian) of the French Jura Mountains: Focus on the factors controlling the formation of microporous facies. *Sedimentary Geology* 230, 21–34. https://doi.org/10.1016/j.sedgeo.2010.06.017

Weissert H. & Erba E. 2004: Volcanism, CO_2 and palaeoclimate: a Late Jurassic–Early Cretaceous carbon and oxygen isotope record. *Journal of the Geological Society* 161, 695–702. https://doi.org/10.1144/0016-764903-087

Westphal H., Munnecke A., Pross J. & Herrle J.O. 2004: Multiproxy approach to understanding the origin of Cretaceous pelagic limestone–marl alternations (DSDP Site 391, Blake-Bahama Basin). *Sedimentology* 51, 109–126. https://doi.org/10.1046/j.1365-3091.2003.00614.x

Wieczorek J. 1988: Maiolica – a unique facies of the Western Tethys. *Annales Societatis Geologorum Poloniae* 58, 255–276.

Wimbledon W.A., Reháková D., Svobodová A., Schnabl P., Pruner P., Elbra T., Šifnerová K., Kdýr Š., Frau C., Schnyder J. & Galbrun B. 2020: Fixing a J/K boundary: a comparative account of key Tithonian-Berriasian profiles in the departments of Drôme and Hautes-Alpes, France. *Geologica Carpathica* 71, 24–46.

Žák K., Košťák M., Man O., Zakharov V.A., Rogov M.A., Pruner P., Rohovec J., Dzyuba O.S. & Mazuch M. 2011: Comparison of carbonate C and O stable isotope records across the Jurassic/Cretaceous boundary in the Tethyan and Boreal Realms. *Palaeogeography, Palaeoclimatology, Palaeoecology* 299, 83–96. https://doi.org/10.1016/j.palaeo.2010.10.038

Electronic supplementary material is available online:

Supplement S1 at https://geologicacarpathica.com/data/files/supplements/GC-77-1-Olveczka_SupplS1.txt
Supplement S2 at https://geologicacarpathica.com/data/files/supplements/GC-77-1-Olveczka_SupplS2.txt
Supplement S3 at https://geologicacarpathica.com/data/files/supplements/GC-77-1-Olveczka_SupplS3.txt
Supplement S4 at https://geologicacarpathica.com/data/files/supplements/GC-77-1-Olveczka_SupplS4.txt